EFFECTS OF VERY HIGH DOSE RATES ON THE
RESPONSE OF CALCIUM FLUORIDE THERMOLUMINESCENT DOSIMETERS

by 6408

JAMES DAVID SMARSH

B. S., University of Kansas, 1961

A MASTER'S THESIS

submitted in partial fulfillment of the

requirements for the degree

MASTER OF SCIENCE

Department of Nuclear Engineering

KANSAS STATE UNIVERSITY
Manhattan, Kansas

1971

Approved by:

Herman J. Donnert
Major Professor

TABLE OF CONTENTS

1. INTRODUCTION 1

2. THEORY 3

2.1. Definition of Terms 3

2.2. The Process of Thermoluminescence 5

3. THERMOLUMINESCENT DOSIMETRY 11

3.1. Glow Curve Peaks 11

3.2. Factors Affecting the Dosimeter Response 11

4. DESCRIPTION OF EQUIPMENT 16

4.1. Dosimeters 16

4.2. Reader Unit 16

4.3. Gamma Cell 22

4.4. Electron Linear Accelerator 22

5. DETERMINATION OF THE CALIBRATION CURVE 28

5.1. Necessity 28

5.2. Equipment and Technique 28

5.3. Experimental Procedure 29

5.4. Analysis of Data and Results 30

5.5. Calibration After the Dose Rate Study 34

6. DESIGN OF THE EXPERIMENT 37

6.1. Guidelines 37

6.2. Radiation Facility 38

6.3. Statistical Design of the Experiment 39

7. EXPERIMENTAL PROCEDURE 44

7.1. Electron Beam Monitoring 44

7.2. Preparation of Samples 44

7.3. Sample Holding Device 45

ILLEGIBLE DOCUMENT

THE FOLLOWING DOCUMENT(S) IS OF POOR LEGIBILITY IN THE ORIGINAL

THIS IS THE BEST COPY AVAILABLE

ILLEGIBLE

THE FOLLOWING DOCUMENT (S) IS ILLEGIBLE DUE TO THE PRINTING ON THE ORIGINAL BEING CUT OFF

ILLEGIBLE

THE FOLLOWING PAGES ARE BADLY SPECKLED DUE TO BEING POOR QUALITY PHOTOCOPIES.

THIS IS AS RECEIVED FROM CUSTOMER.

THIS BOOK CONTAINS NUMEROUS PAGES WITH DIAGRAMS THAT ARE CROOKED COMPARED TO THE REST OF THE INFORMATION ON THE PAGE.

THIS IS AS RECEIVED FROM CUSTOMER.

7.4. Irradiation of Samples 48

7.5. Dosimeter Reading Procedure 50

7.6. Determination of Dose and Dose Rate 50

8. ANALYSIS OF DATA 52

8.1. Pulse Shapes 52

8.2. Electron Beam Energy Spectra 52

8.3. Sorting of the Dosimeters 52

8.4. Data Analysis 57

8.5. Results 58

8.6. Presentation of Results 60

9. DISCUSSIONS AND CONCLUSIONS 62

9.1. Discussion of Results 62

9.2. Previous Investigations and Results 63

9.3. Conclusions 63

10. LIMITATIONS OF THE CURRENT INVESTIGATION 65

11. SCOPE FOR FUTURE WORK 68

12. ACKNOWLEDGMENTS 69

13. LITERATURE CITED 70

14. APPENDIX A (Raw and Computed Data from Irradiation on the LINAC). 72

LIST OF FIGURES

1. Energy band model of a crystal 4

2. A typical glow curve for CaF_2:Mn 6

3. A view of the EG and G model TL-3B thermoluminescent dosimeter reader 18

4. A block diagram of the EG and G model TL-3B reader 19

5. A typical chart record of the EG and G model TL-39 dosimeter. . 20

6. A typical chart record of the EG and G model TL-39 dosimeter after partial annealing 21

7. EG and G model TL-81A read head adaptor and TL-39 dosimeter . . 23

8. A view of the Gammacell-220 24

9. Views of the main control panel of the LINAC 26

10. Views of the auxillary control panel of the LINAC 27

11. Calibration curve for the EG and G model TL-39 dosimeter . . . 33

12. Calibration curve for the EG and G model TL-31 dosimeter . . . 35

13. Planned design of the experiment 41

14. Actual design of the experiment 43

15. A view from the injection end of the LINAC 46

16. Dosimeter sample for irradiation on the LINAC 46

17. Dosimeter sample in self-centering holding device 47

18. A view of the center beam port on the LINAC 49

19. A view of the irradiation assembly on the LINAC 49

20. Typical electron beam pulse shapes for various pulse widths . . 53

21. Typical electron beam energy spectra for various beam currents. 54

22. Typical developed x-ray films 55

23. Typical developed x-ray films 56

24. Response of CaF_2:Mn dosimeters to varying dose and dose rate. . 61

LIST OF TABLES

I. Reduction of standard deviation by use of relative response . . 13

II. Data and results for the calibration curve 31

III. Results of regression analysis 59

IV. Comparison of the calculated uniform dose with the dose obtained from the calibration curve 67

V. Raw and computed data from irradiation on the LINAC 72

1. INTRODUCTION

Shortly after the discovery of x rays and radioactivity, the need for measurement of radiation energy absorbed became apparent. The amount of radiation energy absorbed is known as radiation dose, and the art of its measurement has become known as radiation dosimetry. The hazards of radiation together with its increasing use in medicine, industry, research, and military applications have emphasized the requirements for precise dosimetry during the last two decades.

Since radiation cannot be detected by the senses, radiation dose must be measured indirectly by its effects. Early dosimetry devices consisted of ionization chambers or photographic emulsions. Then "chemical dosimetry" was developed followed by the recent development of "solid-state dosimetry" utilizing the effects of radiation in solids. In some solid materials called phosphors a small fraction of the radiation energy absorbed is stored in metastable energy states. Some of this energy can be recovered later as visible photons of light if the material is heated. This phenomenon of light photons released by thermal means is known as thermoluminescence (TL). TL has been observed for centuries when certain fluorites and limestones have been heated (1).

Thermoluminescent materials have attracted considerable interest in dosimetry because of their following properties:

1. wide range (10^{-4}R up to 10^{8}R)
2. small size
3. sensitivity to all kinds of ionizing radiation
4. accuracy
5. re-usability
6. convenient and quick readout.

They are being used with advantages in the fields of personnel dosimetry, health physics, and research dosimetry. Two main disadvantages are:

1. the difficulty in reproduction of the phosphors arising from extreme sensitivity to minute impurity concentrations.
2. the requirement for complicated and expensive reading devices.

A long list of thermoluminescent phosphors suggested for use in dosimetry is given by Cameron et al (1). Each phosphor is associated with its own advantages and disadvantages. Dosimetry using the synthetic phosphor calcium fluoride manganese (CaF_2:Mn) was first developed by Ginther and Kirk (2) and Schulman et al (3). The specific advantages of CaF_2:Mn as compared to other phosphors are its high sensitivity and near linear response to dose. A disadvantage of this phosphor is its response dependence on energy due to its relatively high effective atomic number.

Although thermoluminescent dosimetry (TLD) can now be considered a well established technique, its fundamental theory is far from understood. All the dosimetry techniques are empirical in that they require calibration with a standard radiation source prior to use. Several factors such as temperature, type of radiation, dose rate, etc., may change when the dosimeters are placed in practical use, and it is necessary to know the effects of all these factors to obtain meaningful results. The primary purpose of this research was to study the effect of high dose rates on the response of CaF_2:Mn TL dosimeters. This effect has been studied by other investigators using dose rates up to 10^{11} rad/sec and doses up to 4,500 rad (4). But considering the increasing scope of application of CaF_2:Mn dosimetry and its potentialities it is now important to know the effect of dose rate at higher values of dose rate and total dose. Studies such as this when considered with other characteristics of the thermoluminescence of CaF_2:Mn may give important clues towards understanding its mechanism.

2. THEORY

2.1. DEFINITION OF TERMS

2.1.1. Radiation Absorbed Dose (rad):

The rad is a unit of absorbed dose and is defined as the absorption of 100 ergs of energy per gram of material (ICRU, 1962). Although the measured thermoluminescence is directly indicative only of the energy absorbed by the phosphor, the TL response may be related to the absorbed dose in other materials by appropriate calibration techniques and correction factors. The conversion factor for converting from material A rads to material B rads is given by:

$$f = \frac{(\mu_{en}/\rho)\ \text{material B}}{(\mu_{en}/\rho)\ \text{material A}}$$

where μ_{en}/ρ is the mass energy absorption coefficient for the material indicated and the type and energy of radiation in question. Unless otherwise specified, all doses in this study will be in units of water rads.

2.1.2. Radiation Thermoluminescence:

Certain types of crystals store energy when they are exposed to ionizing radiation. Upon being heated, they release this stored energy in the form of light. This phenomenon is known as thermoluminescence (TL).

2.1.3. Phosphor:

A material which exhibits TL is often referred to as a phosphor. The term phosphor applies to any material in which the emitted light photon occurs more than 10^{-8} sec after the original energy absorption event. The basis of a phosphor is a pure insulating crystal which is made luminescent by the addition of a small proportion of impurity material referred to as an activator or doping. If the phosphor is used in dosimetric applications, it is called a thermoluminescent dosimeter (TLD).

2.1.4. Traps:

Structural imperfections found frequently in crystals form localized centers of positive or negative charge. For a survey of types of centers, the reader is referred to Schulman (5). These centers are capable of trapping electrons or holes, depending upon the charge they have accumulated. Transitions between the energy levels of these centers result in the absorption or emission of colored light characteristic of the trap. These traps are therefore also known as color centers. The particular center consisting of an electron trapped at an anion vacancy is called an F-center after the German word for color center: "Farbzentrum" (5). The concentration of traps can be influenced by doping with impurities.

2.1.5. Trap Depth:

The electron energy levels associated with the traps are located in the forbidden energy gap between the valence band and conduction band of the ideal crystal. The energy, E_t (Fig. 1) between the lower edge of the conduction band and the energy level of the trap is known as the trap depth because a trapped electron requires energy at least equal to E_t to be lib-

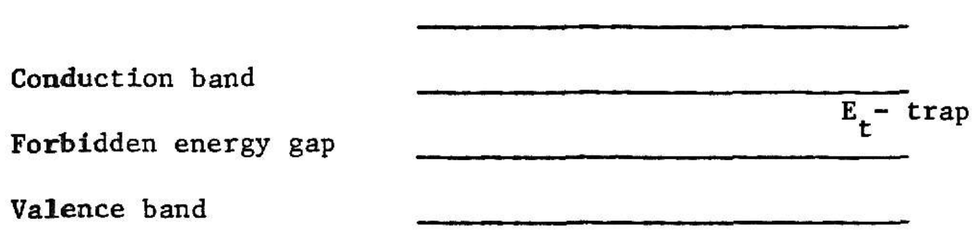

Fig. 1. Energy band model of a crystal.

erated from the trap.

2.1.6. Glow Curve:

As an irradiated phosphor is heated the intensity of light emitted varies with the temperature. A plot of this light intensity as a function of temperature is known as the glow curve. A typical glow curve for CaF_2:Mn (5) is reproduced as Fig. 2.

2.2. THE PROCESS OF TL

The phenomenon of TL is not completely understood even today. The varying shapes of glow curves obtained with different types of phosphors have led people to suggest various models for TL, the validity of any of which is not fully ascertained. However, a simple model of TL can be employed to generally explain the phenomenon.

2.2.1. A Simple Model of TL:

Ionizing radiation upon interacting with an insulating crystal imparts enough energy to electrons to release them from the valence band to the conduction band leaving holes in the valence band. The electrons and holes wander through the crystal until they recombine or until they are trapped in metastable states. These metastable states are assumed to be associated with lattice defects caused by natural imperfection or impurity doping of the crystal. As the dosimeter is heated, a temperature is reached such that the trapped electron acquires enough energy to escape from the trap to the conduction band. The electron may then either be trapped again or fall back to a hole in the valence band emitting one or several photons (TL). An alternative process can occur in which the trapped hole is liberated and migrates via the valence band until it recombines with a trapped electron emitting a TL photon. For dosimetric applications of a phosphor, the TL is assumed to be proportional to the number of trapped electrons which in turn is assumed proportional to the radiation dose received by the phosphor.

This represents an over-simplified picture of TL. The complicated shapes of glow curves obtained from different phosphors suggest that the

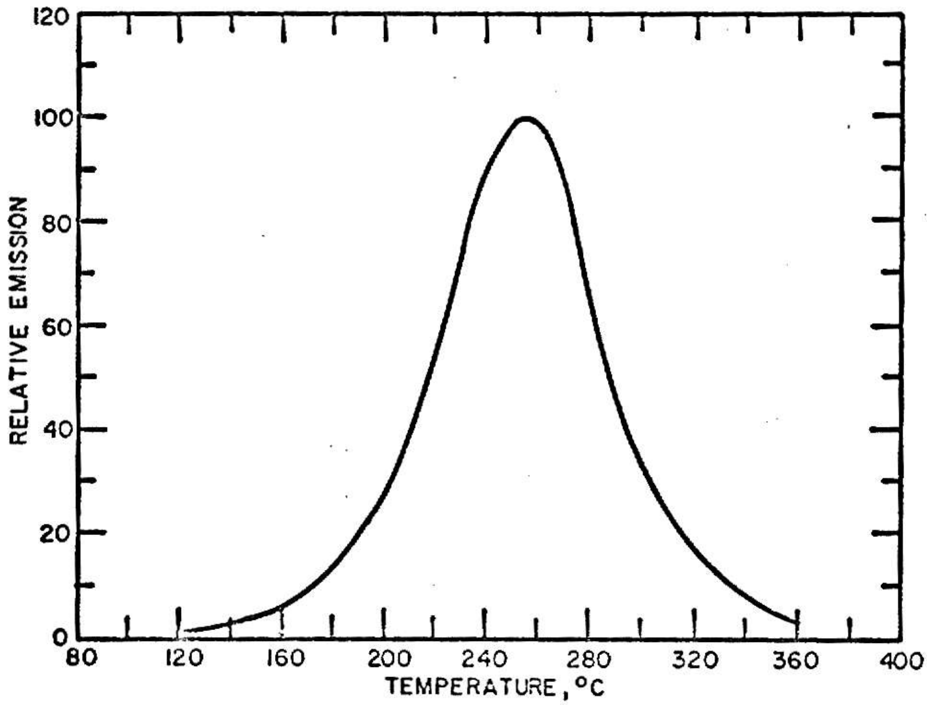

Fig. 2. A typical glow curve for CaF_2:Mn

mechanisms of excitation of electrons, their trapping and their release are more involved. The mechanisms might even be different for different phosphors. A brief description of the theories developed so far to explain the glow curve and some other characteristics of TL is given in the following sections.

2.2.2. Model Suggested by Randall and Wilkins (6):

Randall and Wilkins developed for the first time a mathematical equation for the glow curve. One of the main assumptions they make for developing the model is that the electrons released from the traps have negligible probability of becoming trapped again. As the phosphor is heated, the probability of releasing a trapped electron is related to the trap depth and temperature by an equation of the form of the Arrhenius equation. The TL intensity then increases as electrons are released from the traps by increasing temperature, reaches a maximum, and then decreases as the store of trapped electrons is depleted. For a fixed heating rate, the TL of the crystal is then proportional only to the concentration of trapped electrons. The light emission process is thus suggested to be of first order kinetically. According to this model a peak would appear in the glow curve corresponding to each particular trap depth.

2.2.3. Model Developed by Bonfiglioli et al (7):

Hill and Schwed (8) found experimentally that the activation energy (defined earlier as trap depth) is unique even though several peaks appear in the glow curve of NaCl. From this idea Bonfiglioli et al (7) developed a model for TL which explains the appearance of several glow peaks corresponding to a unique trap depth. They assumed that the electrons released from the traps populate the conduction band. The electrons are then trapped in "luminophor centers," and each glow peak corresponds to a particular type of luminophor center. The TL intensity of light emitted by the crystal then depends not only upon the concentration of trapped electrons but also upon the concentration of luminophor centers, thus making the light emission process second order kinetically.

2.2.4. Model Developed by Cameron et al (9):

In addition to exciting electrons to the conduction band, which later fall into traps, radiation quanta are proposed also to create new traps in the phosphor, thus increasing the total number of empty traps. These "created" traps are expected to bleach out at high temperatures of annealing. For developing some mathematical equations the following assumptions were made: (1) a fixed number of initially empty traps, (2) creation of traps by irradiation with a proportionality constant, (3) filling of traps by irradiation with a proportionality constant, and (4) a maximum number of total traps. For processes that occur during heating the Randall and Wilkins model is assumed to hold.

This is the only model proposed so far which suggests some details of the irradiation process. But with these new ideas more questions arise. Are the proportionality constants for the creation and filling of traps dependent upon the total dose and upon the rate at which the dose is delivered? The answers to these and many other questions are yet to be found.

2.2.5. Predictions of Theory for the Dose Rate Effect:

The primary interest in this investigation was to determine whether or not the TL response of TLD's depends upon the rate at which they are supplied with the dose. In other words, if two identical dosimeters are supplied with the same total dose but at different dose rates, do their responses remain the same? In order to predict this dose rate effect the actual processes occurring in the dosimeter during irradiation must be known.

Unfortunately, the details of such processes are unknown. Most of the models proposed for TL are intended only to explain the glow curve, and as such the details of the irradiation mechanisms are ignored.

Generally the effect of radiation on dosimeters is assumed to be only exciting electrons from the valence band to the conduction band. The total number of electrons trapped and hence the response R of the dosimeter is then proportional to the concentration of electrons in the conduction band n and the concentration of empty traps T:

$$R \sim n \cdot T$$

If T is very large, as generally is the case, it practically remains constant with time especially at low doses. The process of irradiation at low doses then remains pseudo-first-order kinetically. At higher doses it is possible that T changes with time leading to second order kinetics for the process of irradiation. Response in such cases should decrease because a portion of the excited electrons will recombine as the probability of recombination no longer remains negligible compared with the probability of trapping.

If Cameron's model is assumed to be true then the effects of dose and dose rate on the proportionality constants must be known before the dependence of response on dose rate can be predicted.

2.2.6. Dose Rate Dependence vs. Reaction Kinetics:

A theory developed by Donnert (10) and outlined by Kaiseruddin (11) relates the dose rate effect to the kinetic order of the irradiation process. It was shown that:

(1) The response of any dosimetry system to ionizing radiation will exhibit an observeable dependence on dose rate if and only if its reaction mechanism involves any processes which are not kinetically of first order.

(2) An existing dose rate effect for a dosimetry system is necessarily a dose dependent phenomenon; the response of these dosimetry systems must, therefore, be considered as a function of dose and dose rate, two independent parameters.

2.2.7 Mathematical Model for the Dose Rate Effect:

Donnert's theory leads to a mathematical expression for the response which may be tested experimentally. Since the functional relationship between the response R of a dosimeter to a dose D delivered at a dose rate Θ is not known, the response R can be expressed by an nth degree polynomial in D and Θ:

$$R = R_{00} + R_{10}D + R_{01}\Theta + R_{11}D\Theta + R_{20}D^2 + R_{02}\Theta^2 + \dots R_{ij}D^i\Theta^j \qquad (2.2.7\text{-}1)$$

where R_{ij} (i = 0, 1, ..., n; j = 0, 1, ..., n) are the expansion coefficients independent of D and Θ. In an actual experiment it is difficult to obtain sufficient data for determining a large number of expansion coefficients, therefore in this investigation the expression was restricted to the simplest equation which would provide for the existence of interaction between the two variables D and Θ:

$$R = R_{00} + R_{10}D + R_{01}\Theta + R_{11}D\Theta \qquad (2.2.7\text{-}2)$$

The reason why only the interaction term ($R_{11}D\Theta$) has been included out of the three second order terms is evident from Donnert's theory. According to this theory, if the response is dose rate dependent, the dose rate effect is a dose dependent phenomenon which can only be satisfied by a non-zero R_{11} coefficient.

3. THERMOLUMINESCENT DOSIMETRY

3.1. Glow Curve Peaks:

A typical glow curve as cited in the literature is shown in Fig. 2. This glow curve indicates the presence of only a single peak. For the EG and G TL-39 dosimeters, a secondary peak was observed in addition to the primary peak (Fig. 5). The source of this extra peak is not known but was present in all the EG and G TL-39 dosimeters used in this research. It is suspected that some minute impurity doping may be the source.

3.2. Factors Affecting the Dosimeter Response:

Although much research work has been and is being done on TL dosimetry, standard methods of dosimetry have not yet been established. Some of the factors that affect the response critically along with the reasons for selecting particular methods in this research are discussed in the following sections.

3.2.1. Types of Radiation:

Pinkerton et al (12) compared the response of LiF TL dosimeters to ^{60}Co gamma rays with that to 10 and 15 MeV electrons. They reported the following response ratios when the same amount of dose was supplied in all cases:

$$\frac{\text{Response to 15 MeV electrons}}{\text{Response to }^{60}\text{Co gamma rays}} = 0.893 \pm 0.018$$

$$\frac{\text{Response to 10 MeV electrons}}{\text{Response to }^{60}\text{Co gamma rays}} = 0.876 \pm 0.021$$

The response to different types of radiation differed by a constant factor, but the shapes of glow curves obtained for different heating times remained the same in all cases. This indicates that the final effects of the interaction of high energy electrons with LiF are the same as those in the case of ^{60}Co gamma rays, but only slightly less in magnitude. It was on this basis that 15 MeV electrons were chosen for the primary study of this investigation of the CaF_2:Mn dosimeters.

3.2.2. Physical Characteristics of the Phosphor:

Obviously, larger amounts of phosphor will store larger amounts of energy and hence will give higher response. But this also depends upon the physical arrangement of the phosphor when it is heated. If it is arranged in a thick layer, the layers at the top may screen the light emitted by the layers at the bottom, thus affecting the total light measured. Due to small fluctuations in the weight of the phosphor, grain size, geometry of ampule, and phosphor sensitivity, the response of individual dosimeters in a batch will vary. In order to determine the approximate extent of this individual variation, two groups of 15 dosimeters were irradiated to a reference dose of 975 rad to obtain an individual dosimeter reference response. The dosimeters of group I and group II were then irradiated to doses of 10,414 and 14,274 rad respectively. The mean response and standard deviation for each group were calculated. The response of each dosimeter was then divided by its reference response to obtain its relative response. The mean relative response and standard deviation of groups I and II were then computed and compared with the non-relative response values. The results are tabulated in Table I. As can be seen, the relative response can be used to reduce the percentage standard deviation of the response of a group of dosimeters by approximately 50 %.

Table I. Reduction of standard deviation by use of relative response.

Group	Mean response	Standard deviation	Percentage of mean	Mean relative response	Standard deviation	Percentage of mean
I	367.4	51.13	13.9	11.76	0.695	5.9
II	570.5	92.45	16.2	16.96	1.497	8.9

3.2.3. Quantity Taken to Represent Response:

Strictly speaking the total light emitted by the dosimeter during the complete heating cycle, which is equal to the area under the TL glow curve, gives the response which is proportional to the radiation dose. But in practice use of this quantity has a disadvantage. At high temperatures the heating element also emits infrared light and at low doses the main radiation induced peak ($\sim 280^{\circ}C$) is quickly followed by a nonradiation-induced tribo-thermoluminescent peak ($350^{\circ}C$) which is induced in loose powder by mechanical handling (13). Thus it becomes difficult to decide at which point the integration should be discontinued in order to measure only the radiation induced TL.

It has been found that when the heating cycle is reproducible the glow peak heights are also proportional to the radiation dose supplied. Therefore when this response is taken as a measure of dose the disadvantage of the light sum method is avoided (5).

3.2.4. Method of Annealing:

The necessity for annealing dosimeters before reuse arises from the fact that all the traps are not fully depopulated by the small heating cycle of the TLD reader. However, the method of thermal annealing affects the response of TL dosimeters (14). It is, therefore, quite important that a suitable annealing procedure be adopted and adhered to for consistent results.

EG and G has recommended that TL-39 dosimeters exposed to doses of the order of 50,000 rad be annealed at 350°C for 5 hours or until the response of a dedosed dosimeter is less than 0.0005 reader units (15).

3.2.5. Heating Rate:

The shape of the glow curve is highly dependent upon the heating cycle used in reading the dosimeter. The true shape of the glow curve is obtained only when the rate of temperature rise is constant. Changing the heating rate has several effects on the response. If the heating rate is increased the peaks in the glow curve appear at higher temperatures and the peak heights decrease at heating rates greater than 30°C/min (1).

Constant rate of temperature rise is not necessary in dosimetry, but reproducibility of the heating cycle is required for the results to be consistent. The EG and G reader used in this work used a heating cycle which produced a nearly constant rate of temperature rise, and a heater coil arrangement which insured reproducibility of the heating cycle.

3.2.6. Fading:

To function as a satisfactory dosimeter, a phosphor should have a TL response that is independent of the storage time at room temperature between exposure and reading.

3.2.6(a). Theoretical Background:

Phosphors containing shallow traps produce responses which fade much faster than those containing deep traps, and hence are not suitable for dosimetry purposes. Phosphors containing both shallow and deep traps present some potential problems connected with fading which must be avoided. Effects of fading that may be expected in such phosphors are:

1. a reduction in the total light output due to the escape of electrons from shallow traps,

2. an increase in the height of the high temperature peaks due to some of these escaped electrons falling into deeper traps (assuming that the high temperature peaks are caused by deeper traps).

If the peak height of the high temperature peak is taken to give the response the first effect does not create any problem; however, positive measures must be taken to prevent the second effect from affecting the results.

3.2.6(b). Previous Investigations:

Alexander (16) studied the fading effects on the glow peak height response of EG and G TL-31 CaF_2:Mn dosimeters. He found that partial annealing of the dosimeters for 7 min at 161°C following irradiation removed the low temperature peak and reduced the spread of the response data. He also found using this technique that no significant fading effects were present up to 100 hours following irradiation. Therefore this annealing procedure was adopted in this investigation. Glow curves for the TL-39 dosimeters without and with partial annealing are reproduced in Figs. 5 and 6.

4. DESCRIPTION OF EQUIPMENT

4.1. Dosimeters:

EG and G model TL-39 "CaF_2:Mn Microthermoluminescent Dosimeters" were used in this study (Fig. 7). The dosimeters consisted of 0.8 mg of CaF_2:Mn phosphor hermetically sealed in a glass capillary tube. The dosimeters were 0.9 mm in diameter and 6.0 mm in length. The EG and G batch number was 10-4-68.

The following characteristics of the dosimeters were reported by the manufacturer (15). The useful range of the dosimeters was reported as 1 R to 10^5 R. Dosimeters were reported to give a linear response with respect to dose within 3 %. Response was reported dependent upon the energy of the radiation, but was independent of ordinary ambient temperature changes.

Reproducibility of the dosimeters was reported to be within 3 %. Due to small fluctuations in the weight of the phosphor, grain size, geometry of ampule, and phosphor sensitivity, the responses of the dosimeters from a batch selected by the manufacturers were reported to be within 10 % of the mean. No dependence on dose rate was reported for dose rates below 10^9 R/sec.

4.2. Reader Unit:

An EG and G model TL-3B reader (Fig.3) was used to read the dosimeters. Basically the reader unit heated the dosimeter, supplied the light emitted to a photomultiplier (PM) tube, and used the output signal of the PM tube to drive a chart recorder which produced a glow curve.

A block diagram of the reader unit circuitry is shown in Fig. 4. The regulated current supply fed the read head adapter (described below) in which the dosimeter was positioned. Light emitted by the dosimeter was reflected towards the PM tube. The output signal of the PM tube was fed to a pen-servomechanism in the recorder unit via an automatic ranging circuit. Initially the PM tube was set to its maximum sensitivity, which gave the lowest response range on the recorder. When the light output increased beyond this range and the pen reached full scale on the recorder, the automatic ranging circuit lowered the reader sensitivity by a factor of 10. In this way readings from the lowest full scale range of 0.050 reader units to the highest full scale range of 5,000 reader units were possible. The control logic sequenced the operations of the recorder, detector heating cycle, automatic ranging circuits and the status indicator to provide a chart record of the light emission from the dosimeter. The status indicator gave the full range of the recorder.

A standard ^{14}C source, whose light output was equivalent to 0.340 reader units with the TL-32A reference dosimeter, was provided for calibration of the reader unit. The calibration was accomplished by changing the high voltage across the PM tube. The normal useful range of the reader was 0.050 reader units to 5,000 reader units with the standard dosimeter, but it could be extended down to 0.005 reader units or up to 50,000 reader units by respectively increasing or decreasing the gain of the PM tube.

Typical chart records obtained on this reader with the TL-39 dosimeters are reproduced in Fig. 5 and Fig. 6. The heater turned on when the pen reached the short line at the base near the middle of the chart and turned off at the end of the chart. Each time the range switch operated, the event marker pen produced a vertical "pip" in the continuous line at the top of the chart. Thus the final range of the recorder could be determined by counting the number of "pips", besides observing it on the status indicator.

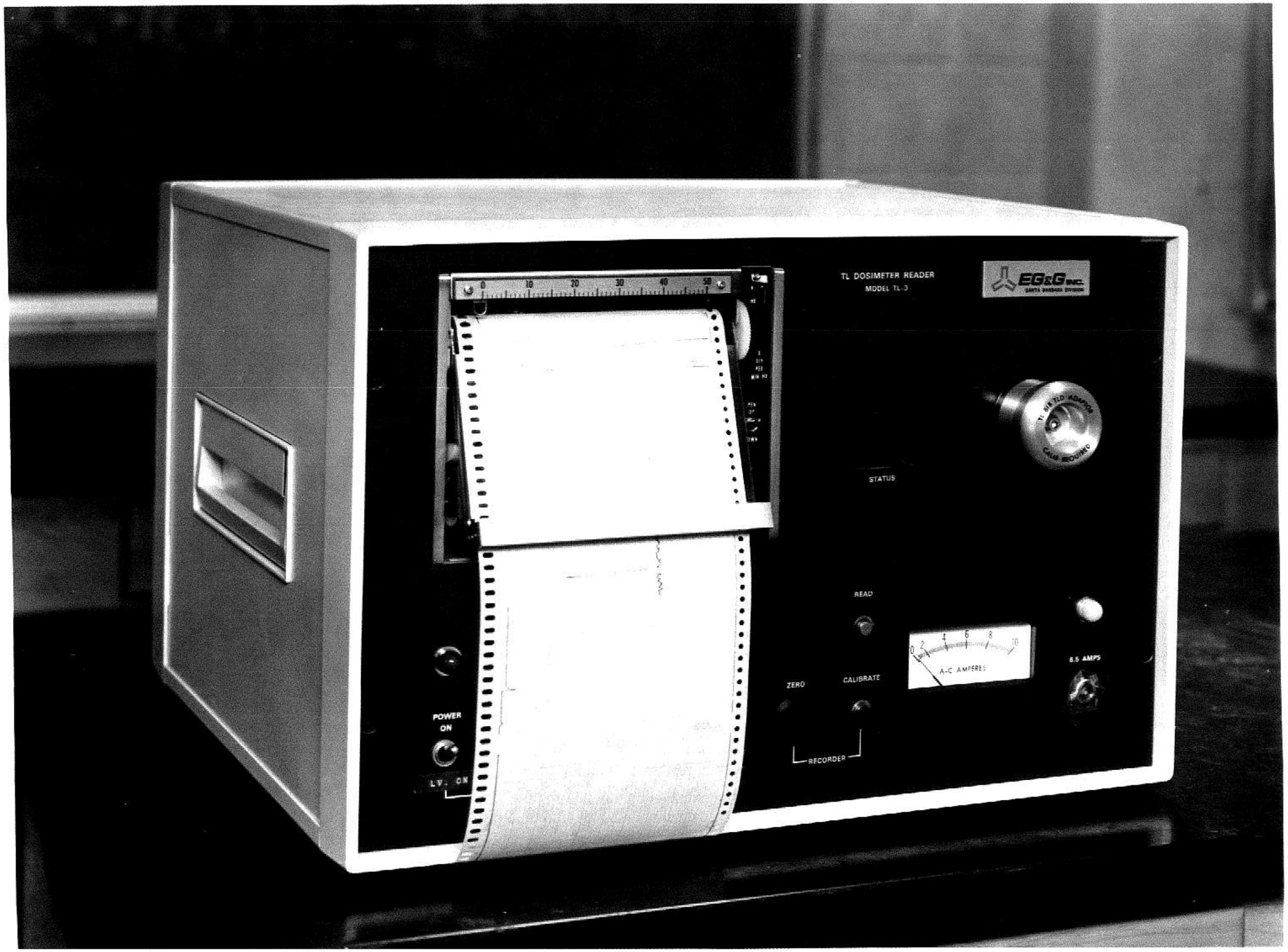

Fig. 3. A view of the EG and G model TL-3B thermoluminescent dosimeter reader.

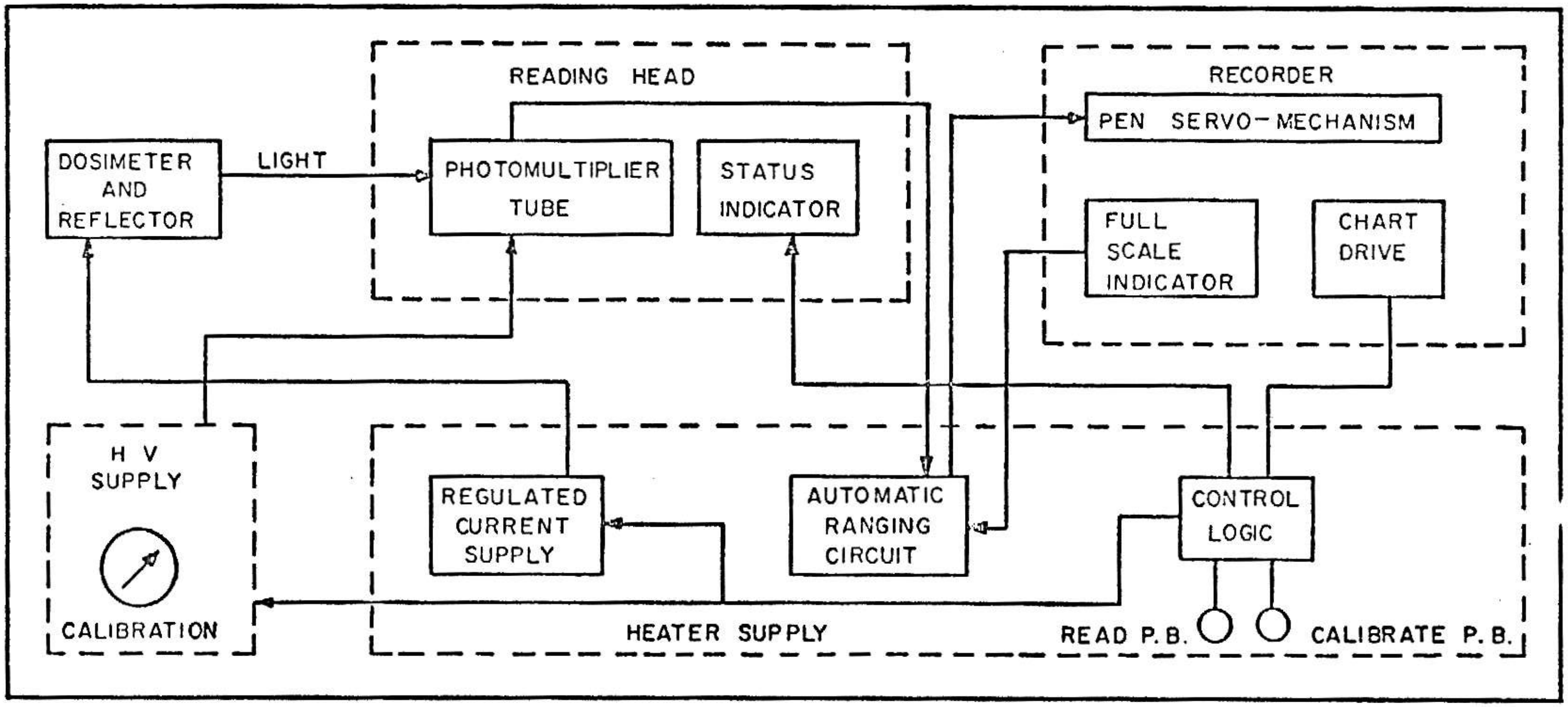

Fig. 4. A block diagram of the EG and G model TL-3B reader.

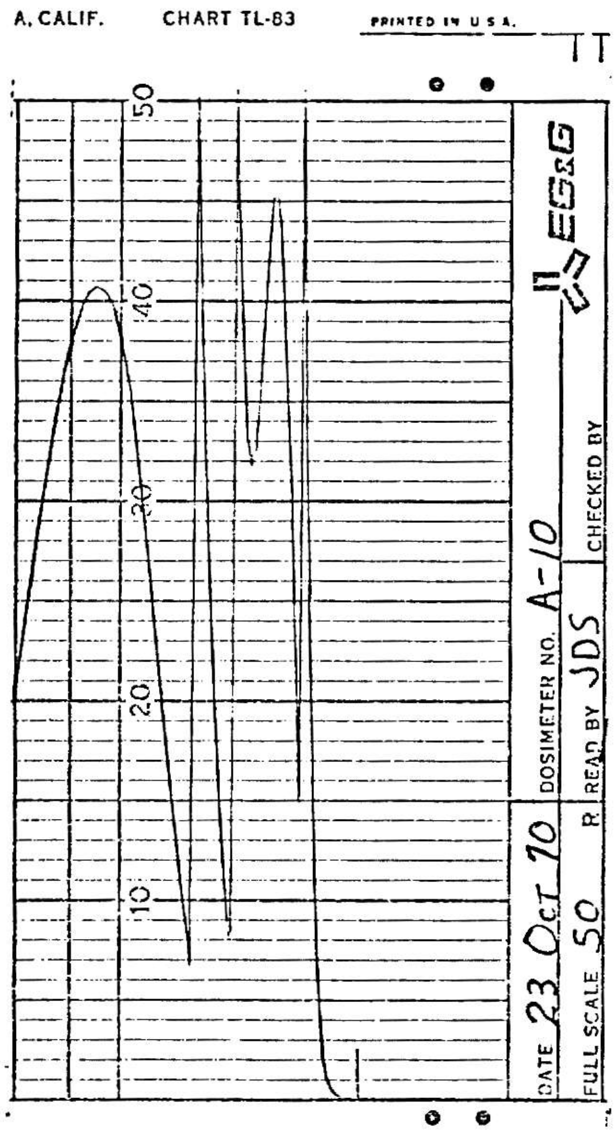

Fig. 5. A typical chart record obtained from the TL-39 dosimeter.

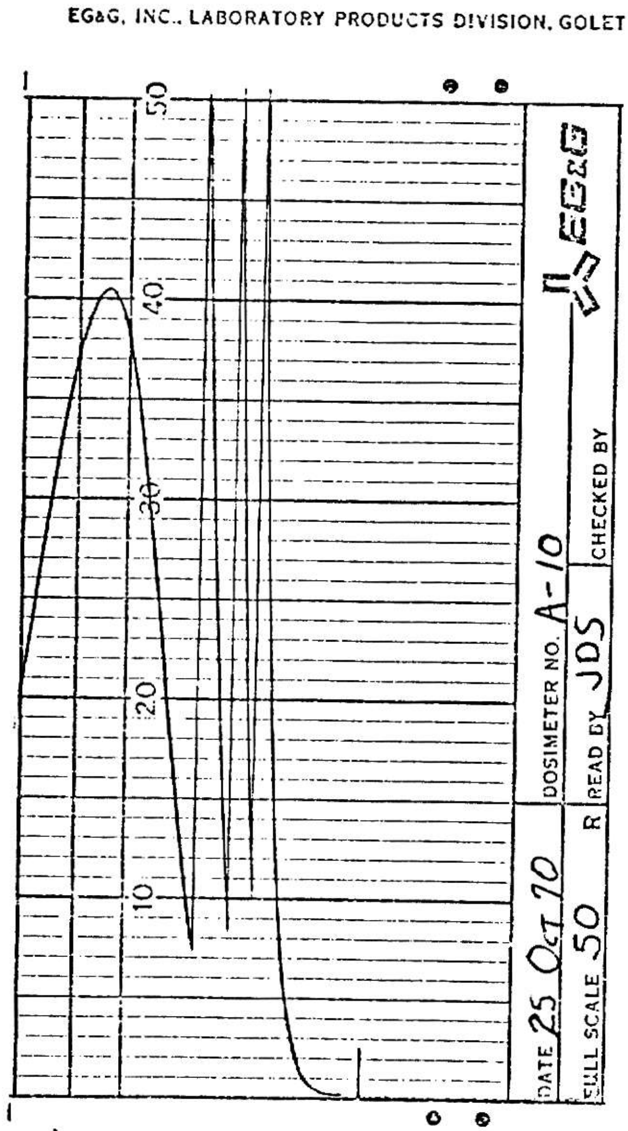

Fig. 6. A typical chart record obtained from the partially annealed TL-39 dosimeter.

An EG and G Model TL-81A read head adapter (Fig. 7) was used to hold and heat the model TL-39 dosimeters in the reader unit. It consisted of a heating coil and a shunt resistance. It received a constant current of 6.5 A from the regulated current supply. The shunt resistance could be adjusted such that a correct amount of current, which would produce the glow peak in the middle of the three lines to the left of the chart (see Fig. 5), flowed through the heating coil.

4.3. Gammacell:

A Gammacell-220 manufactured by the Atomic Energy of Canada Ltd. was used to calibrate the dosimeters. The gammacell was loaded with a 3,963 Ci ^{60}Co cource on March 15, 1965. The source was in the form of a hollow circular cylinder located inside a thick water shield. A 6-inch diameter by 8-inch irradiation chamber was located in a plunger, which lowered it into the middle of the source. The plunger was operated by an electronic timer which could be set for seconds, minutes, or hours. The Gammacell-220 is shown in Fig. 8.

4.4. Electron Linear Accelerator:

For obtaining very high dose rates of the order of 10^{10} to 10^{12} rad/sec the electron linear accelerator (LINAC) at the Argonne National Laboratory was used. The specifications of the LINAC for the electron energy pertinent to this study (15 MeV) were the following. The peak beam current was 10 amperes. For a beam current less than 2 amperes, the pulse length was continuously variable from 0.006 to 10 μsec. For beam currents greater than 2 amperes, the pulse length capability was limited to 0.006, 0.008, 0.010, 0.020, 0.050, and 0.100 μsec.

To monitor the actual pulse of high energy electrons supplied by the

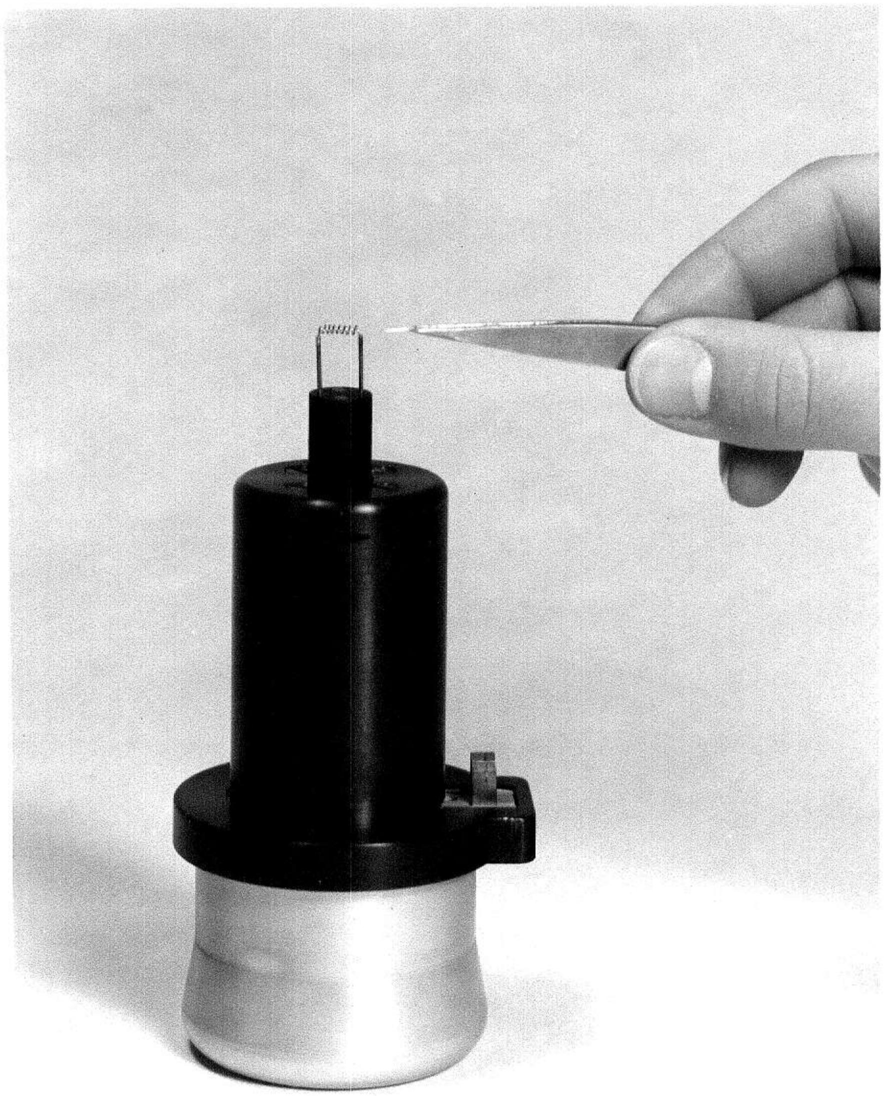

Fig. 7. EG and G model TL-81A read head adapter with TL-39 dosimeter held by forceps.

Fig. 8. A view of the Gammacell-220.

LINAC a Faraday cup was mounted behind the dosimeters to collect the entire beam of electrons. The charge from the Faraday cup was fed to a 10 μF capacitor which in turn was connected to an oscilloscope and a digital voltmeter via an electrometer. A poloroid camera was mounted on the oscilloscope to obtain photographs of the pulse traces produced by the electron beam. The LINAC was operated from the main control panel (Fig. 9) by licensed operators of the Argonne National Laboratory. An auxillary control panel (Fig. 10) consisting primarily of the oscilloscope, the digital voltmeter, and a pulse trigger was provided for the experimenters. A photograph of the LINAC is provided in Fig. 15.

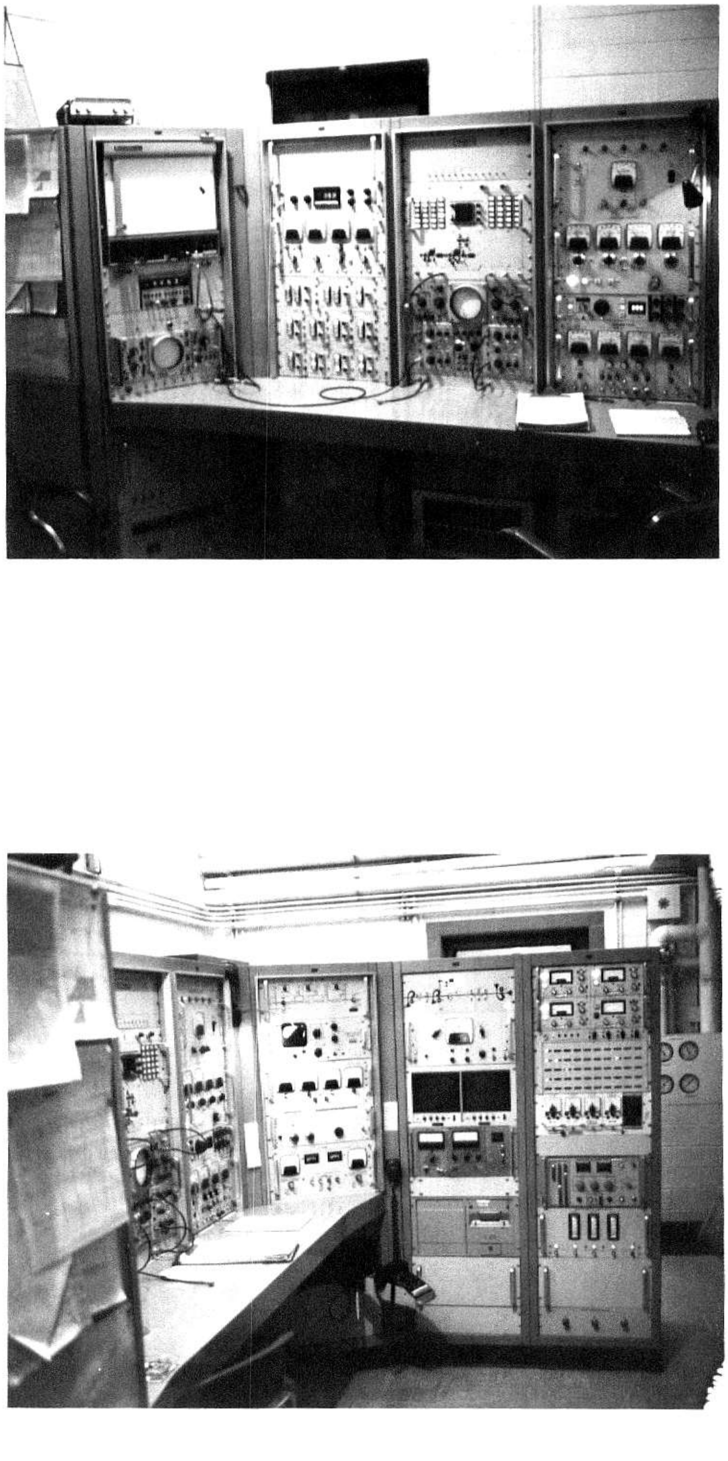

Fig. 9. Views of the main control panel of the LINAC.

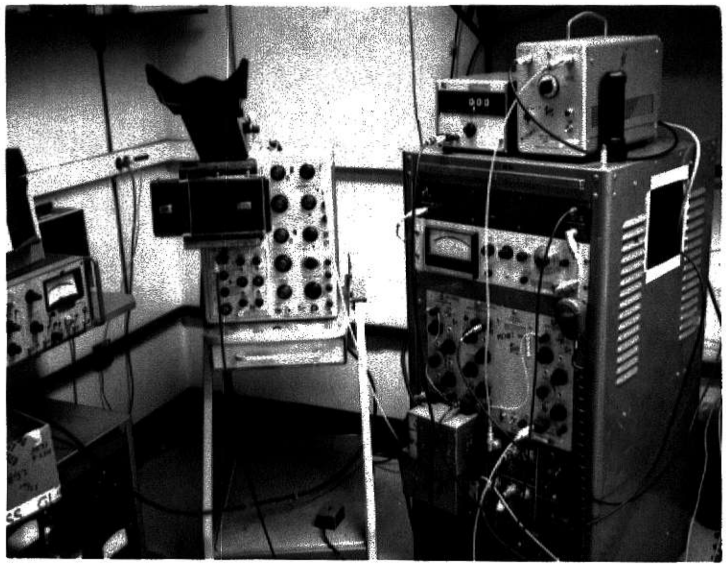

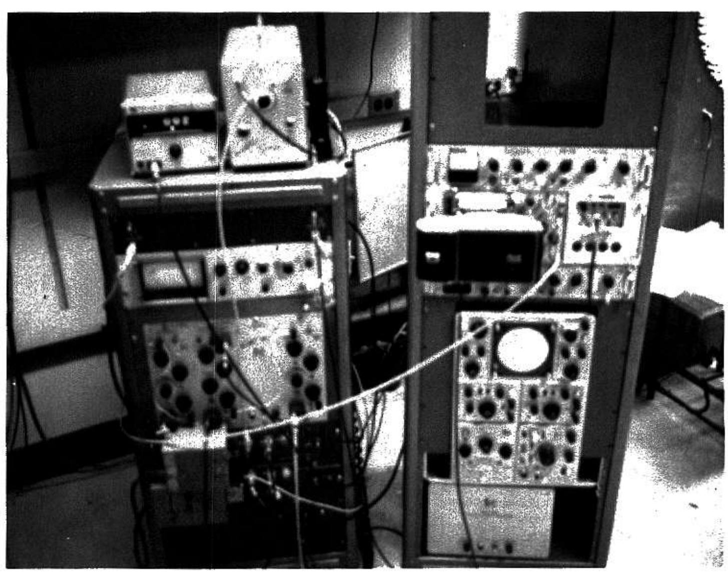

Fig. 10. Views of the auxillary control panel of the LINAC.

5. DETERMINATION OF THE CALIBRATION CURVE

5.1. Necessity:

The peak height measured on the glow curve plotted by the EG and G reader gave the response of the dosimeters in reader units. Due to the supralinearity affect (16), a full calibration curve is required to convert from reader units to radiation dose.

5.2 Equipment and Technique:

The gammacell was used to irradiate the dosimeters for the calibration. The dosimeters were placed on the circumference of a two-inch diameter circle concentric with the outer diameter of a polyethylene disk about ½ inch thick. The disk was constructed to exactly fit in the irradiation chamber and allowed for 24 dosimeters to be irradiated at one time. All dosimeters received the same dose due to their placement on an isodose curve. The disk provided a consistent positioning and holding device for uniformity in all irradiations. The isodose curve as supplied by the manufacturer was 2.75 inches above the base of the chamber and two inches from the vertical axis in order to receive the dose equivalent to the dose at the center of the chamber. Polyethylene was used on account of its low absorption coefficient for gamma rays and because the disk had already been constructed for use by previous experimenters. The disk with the dosimeters positioned in the gammacell is shown in Fig. 8.

The timer equipped on the gammacell was used to time the irradiation. The timer measured the time the plunger was at its lowest position only. Therefore, not only did the dosimeters receive a dose during the pre-set time, but also some constant travel dose while the plunger was traversing down and up. Since the traverse time was constant, a constant travel dose,

D_o, was received in addition to the dose received during irradiation for the pre-set time. Thus total dose, D, was given by:

$$D = D_o + \dot{D}t \qquad (5.2\text{-}1)$$

where $\dot{D}$ is the dose rate in rad and t is the length of time irradiated.

Over the linear portion of the calibration curve (0 to 10^3 rad), the total response, R, of the dosimeters in reader units was given by:

$$R = R_o + \dot{R}t \qquad (5.2\text{-}2)$$

where R_o is the constant response due to traversing down and up in the cylinder and $\dot{R}$ is the dose rate of the gamma source in reader units. A weighted least squares analysis of the experimental data was used to obtain estimates of R_o and $\dot{R}$. The calibration factor, cf, in units of rad/reader unit could then be determined by dividing the known value of the dose rate of the gammacell, $\dot{D}$, by the determined value $\dot{R}$. For the linear region the total dose received in rad could be obtained by multiplying the total response times the calibration factor. Thus, the value for D_o could be determined by multiplying R_o times the calibration factor.

5.3 Experimental Procedure:

To obtain the calibration curve in the wide dose range from 100 rad to saturation (about 1 Mrad) the experimental points were chosen to be fairly equally distributed along the arithmetic scale of dose. The 360 dosimeters reserved for the primary experiment were used in the dose range below 10^5 rad, leaving 40 dosimeters for use in the saturation dose range. All 360 dosimeters were placed in a graphite holder and simultaneously annealed at 350^oC for 5 hours before irradiation. Twenty dosimeters were irradiated simultaneously for each experimental point below 10^5 rad and ten dosimeters per point were used above 10^5 rad. After the 360 dosimeters were irradiated for the appropriate times, all were simultaneously subjected to a partial annealing at 161°C for 7 min.

5.4. Analysis of Data and Results:

For each experimental point, the mean response value and standard error of the mean were calculated. These values are presented in Table II. The first six data points were used in the linear regression for estimating R_o and $\dot{R}$. The values obtained from the linear regression were $R_o = 4.055$ reader units and $\dot{R} = 1.525$ reader units/sec. The calibration factor was obtained by dividing the known dose rate of 42.92 rad/sec by $\dot{R}$. Thus, the value obtained for the calibration factor was 28.15 rad/reader unit. The calibration factor was valid for the linear portion of the response in the low dose range from approximately 100 to 10,000 rad only.

The calibration factor times R_o (the value obtained by linear regression) gave the travel dose, D_o, as 114.0 rad. The timed dose was the dose rate multiplied by the irradiation time. The total dose, D, was obtained by adding the travel dose to the timed dose (Eq. 5.2-1). These values are presented in Table II. In Fig. 11, the total dose is plotted as the abscissa and the experimentally determined response as the ordinate to give the full calibration curve.

The calibration curve indicated supralinearity of response (an essentially nonlinear effect) with respect to dose above approximately 10^4 rad. To obtain a better idea of the supralinearity, the calibration curve was divided into three dose ranges; the low dose range (0 to 10^4 rad), the intermediate dose range (10^4 to 10^5 rad), and the saturation dose range (10^5 to 10^6 rad). The curve shown in Fig. 11 was obtained as follows. In the low and intermediate dose ranges the data were fitted to a linear model

Table II. Data and results for the calibration curve.

Sample number	Duration of irradiation, min	Timed dose, rad	Total dose, rad	Response, reader units
1	0.000	0	114.0	4.04 ± 0.12
2	0.083	214.6	328.6	11.95 ± 0.65
3	0.167	429.2	543.2	19.43 ± 0.73
4	0.250	643.8	757.8	26.68 ± 0.96
5	0.333	858.4	972.4	37.23 ± 1.25
6	0.416	1,073	1,187	39.76 ± 1.30
7	0.667	1,717	1,831	70.45 ± 2.06
8	1.00	2,575	2,689	94.95 ± 2.98
9	1.67	4,292	4,406	156.3 ± 7.1
10	2.3	5,920	6,034	237.9 ± 18.1
11	3.0	7,725	7,839	271.0 ± 11.1
12	4.0	10,300	10,410	367.4 ± 11.4
13	5.5	14,160	14,270	570.5 ± 20.7
14	6.5	16,730	16,840	630.0 ± 19.9
15	8.0	20,600	20,710	855.5 ± 31.2
16	9.5	24,450	24,560	1,073 ± 36
17	11.0	28,300	28,410	1,158 ± 37
18	13.0	33,450	33,560	1,471 ± 41
19	15.0	38,600	38,710	1,776 ± 56
20	20.0	51,500	51,610	2,320 ± 65
21	30.0	76,500	76,600	3,307 ± 155
22	40.0	101,000	101,100	4,378 ± 277
23	60.0	151,000	151,100	6,150 ± 197
24	80.0	202,000	202,100	7,860 ± 402

Table II. (Continued)

25	160.0	404,000	404,100	12,440	±	622
26	240.0	606,000	606,100	15,130	±	699
27	400.0	1,010,000	1,010,000	15,810	±	747
28	600.0	1,510,000	1,510,000	15,580	±	686

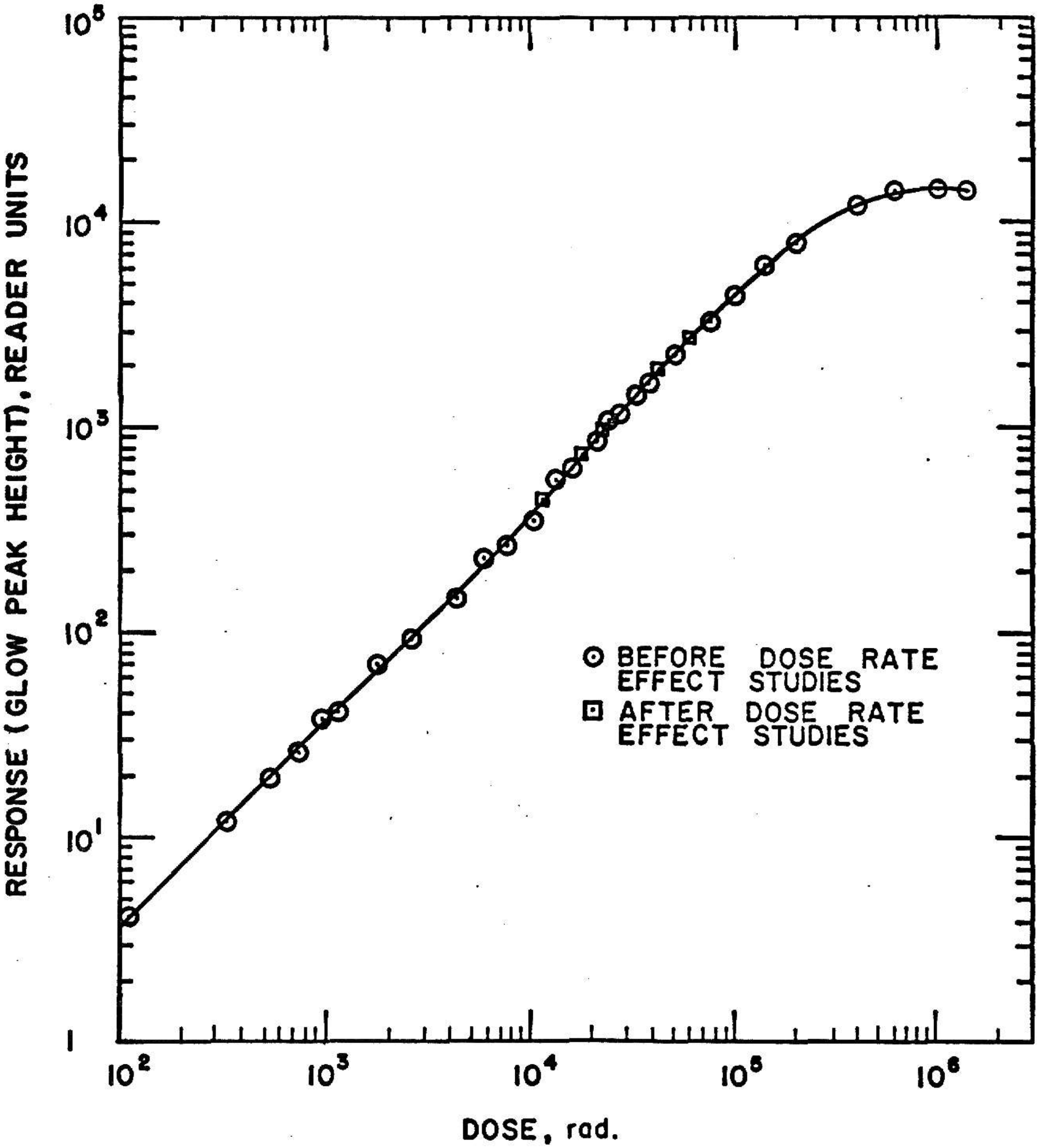

Fig. 11. Calibration curve for the EG and G model TL-39 dosimeter.

in each range using a weighted least squares analysis. In the saturation range a smooth curve was drawn. The linear equation obtained for the low dose range was $R = 0.0359\ D - 0.0379$ and for the intermediate dose range was $R = 0.0469\ D - 123$. The supralinearity is not vividly illustrated by the logarithmic scales, however, the equations indicate that the slope of the curve in the intermediate dose range is 1.3 times the slope in the low dose range. Evidence of saturation began at about 10^5 rad with complete saturation occurring at about 6×10^5 rad.

Comparison of this calibration curve with that obtained by Alexander (16) for the EG and G model TL-31 CaF_2:Mn Minithermoluminescent Dosimeter shows some interesting features. He found supralinearity to begin at approximately 10^3 rad with complete saturation at about 10^5 rad. Also, he found that the slope of the curve in the intermediate dose range was twice the slope in the low dose range. His calibration curve is reproduced in Fig. 12. For comparison purposes it should be kept in mind that Alexander used a larger model dosimeter, a different read head adapter, and expressed his dose in CaF_2:Mn rad (1 water rad = 0.868 CaF_2:Mn rad).

5.5. Calibration After the Dose Rate Study:

Dosimeters were used in the dose rate study near the limit of their useability, hence it was considered that they might develop permanent lattice defects changing their characteristics. To determine whether this had occurred the 40 dosimeters whose response values were used in the dose rate study were irradiated in the dose range of 10^4 to 6×10^4 rad and their response values were plotted in Fig. 11. The close agreement between these points and the calibration curve indicated that no permanent defects were created in the phosphor. It was noted, however, that ten hours of annealing at 350°C was required before the dosimeter responses agreed with

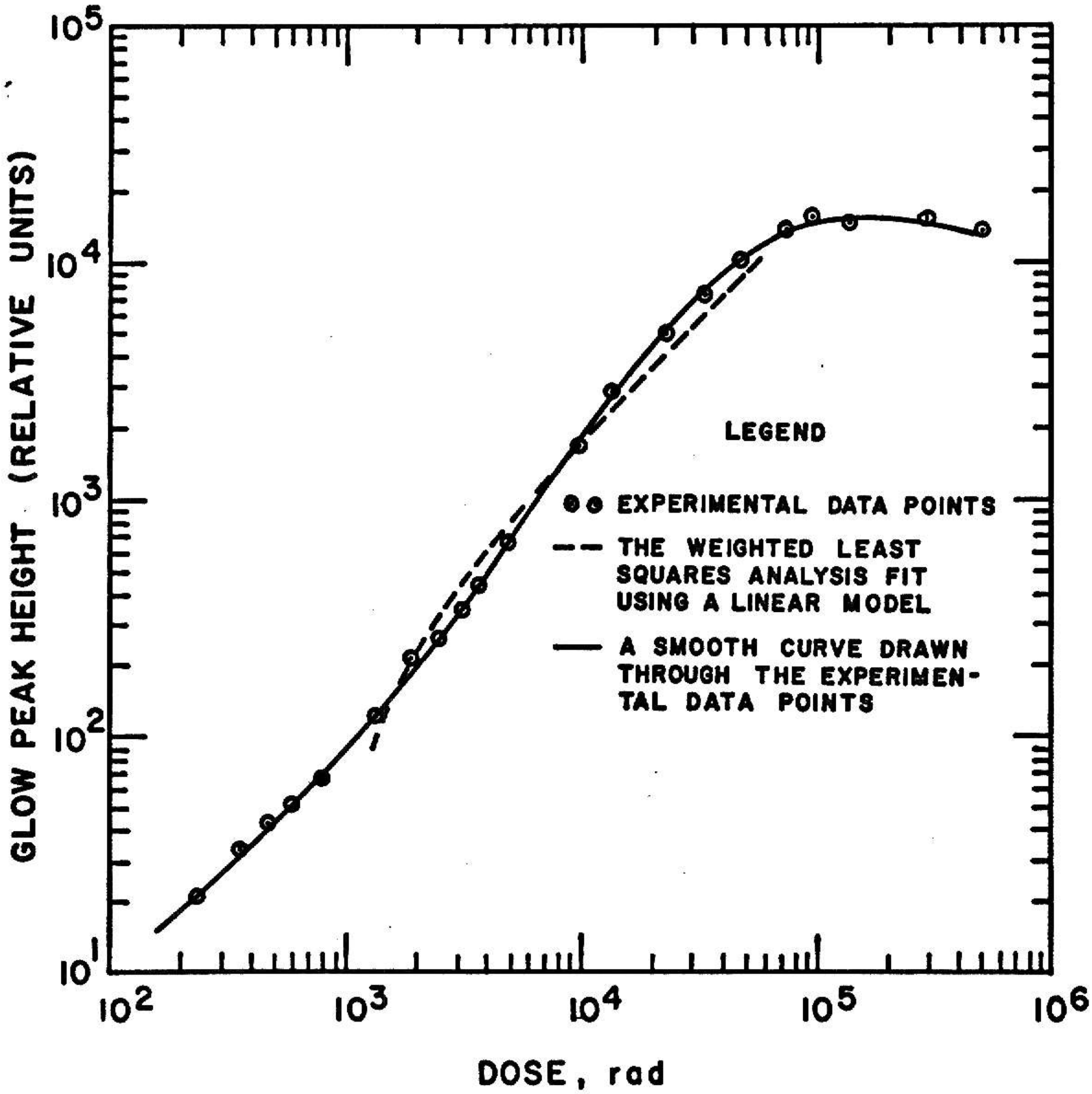

Fig. 12. Calibration curve for the EG and G model TL-31 dosimeter.

the calibration curve.

6. DESIGN OF THE EXPERIMENT

6.1. Guidelines:

As indicated earlier, the primary objective of this work was to investigate whether or not the response of CaF_2:Mn TL dosimeters is dependent upon the dose rate at which the radiation dose is delivered to them. This could have been predicted from theory had the mechanism of the TL of CaF_2:Mn been known. Since the mechanism was not known, the phenomenon had to be investigated experimentally. However, guidelines for the design of the experiment were obtained from any theory or data available.

The only theory which discussed the dose rate dependence of the response was Donnert's theory referred to in sec. 2.2.6. This theory suggested that the response of a dosimeter would be dependent upon the rate at which the radiation dose was delivered and that this dependence would be characteristic of the total dose only if the processes involved in the irradiation were not all of first order kinetically. This would be true, in principle, at any value of the dose rate and any amount of the total dose, but the phenomenon might not be of observeable magnitude in an actual experiment. To increase the probability that the phenomenon would be observeable it seemed necessary to irradiate the dosimeters at very high dose rates and high levels of total dose. Tochilin and Goldstein (4) found no dose rate dependence for CaF_2:Mn in a study using dose rates up to 10^{11} rad/sec and doses up to 4,500 rad. But a similar experiment observed dose rate dependence of film and glass dosimeters, using dose rates in the range of 10^9 to 5×10^{10} rad/sec (1 to 50 krad/μsec) and doses in the range of 6.5 to 48.0 krad. Another similar study (11) found dose rate dependence in LiF TL dosimeters using dose rates in the range of 10^9 to 3×10^{10} rad/sec and doses in the range of 6 to 50 krad.

6.2. Radiation Facility:

There were two primary requirements of the radiation facility to be used in this experiment. First, it should provide gamma radiation or some radiation which is practically equivalent to gamma radiation. Second, it should be capable of providing radiation dose at a rate in the desired range of 10 to 1,000 krad/μsec (10^{10} to 10^{12} rad/sec). In addition there was one more requirement set for the radiation facility by the type of dosimeters selected for use in the experiment. The model TL-39 dosimeters were capable of use in the dose range from 1 to 10^5 rad. For a total dose not exceeding 8×10^4 rad at a dose rate as high as 1,000 krad/μsec the irradiation time should be no longer than about 0.08 μsec. It must be even smaller for obtaining lower total doses at the highest dose rate. Therefore, the radiation facility should be capable of producing radiation in the form of intense, accurate and measureable pulses of 0.01 μsec or less in width.

The high dose rates of interest were not obtainable from any radioisotopes or any other available sources of gamma radiation. The electron linear accelerator, described in sec. 4.4, available at the Argonne National Laboratory was found to be a suitable radiation facility for the purpose of this experiment. The specifications of the LINAC pertinent to this study were given in sec. 4.4. The 15 MeV electrons produced by the LINAC were considered a promising substitute for gammarays, as the difference in response of the dosimeters to these two types of radiation was expected to be slight (sec. 2.2.1.).

The total radiation dose supplied by the LINAC was in the form of a single pulse. The pulse width was measured in units of μsec. The arrangement used to obtain a trace of the pulse shape was described in sec. 4.4. The digital voltmeter would enable computation of total charge in a pulse supplied by the LINAC in units of nC (10^{-9} coulombs). The total dose delivered would be proportional to the total charge supplied and the dose rate could be obtained by dividing the dose by the pulse width. The conversion factor from delivered charge to dose was obtained from Donnert et al (10) to be 0.227 krad/nC. This conversion factor was originally determined by dose measurements with the standard Fricke dosimeter for which the dose and dose rate dependent response was known.

6.3. Statistical Design of the Experiment:

Statistical design of the experiment consisted of determining approximate values of the controlled variables in the experiment, so as to obtain statistically significant results. There were two independent controlled variables in this experiment; namely the total dose D and the dose rate Θ. The mathematical model selected for the analysis of the response R of the dosimeters was given by Eq. (2.2.7-2) which indicated that four constants were to be evaluated. Theoretically, measurement of response at four properly chosen combinations of D and Θ would suffice for the determination of the four constants. But since the proposed model might not be the true relationship between R, D, and Θ, one would be interested in knowing the statistical significance of the fit obtained. This required measurement of response at more than four different combinations of D and Θ.

In selection of different combinations of D and Θ several factors could be taken into account, such as: good fit over the broadest range of interest of the controlled variables, ease in data analysis, and practical feasibility. Importance of all these factors is discussed in several text books on statistics. Various experimental designs are also suggested for various models based upon these factors. An excellent brief discussion may be found in the reference by Hunter (17). A standard design suggested for a full second order model is a 3^2 factorial design in the controlled variables. A multiple of this design was selected for our incomplete second order model to allow for mishaps such as the beam meandering experienced by Kaiseruddin (11). The original design shown in Fig. 13 would provide for the 3^2 factorial design using any 3 of the 5 planned dose rates.

The broadest readily obtainable operating conditions of the accelerator were utilized. It was intended to supply three different dose levels, each at five different amperage settings. This amounted to supplying dose at three different levels each at five different dose rates. The dose levels were set at about 10, 45, and 90 krad. The pulse widths (μsec) required at the planned dose rates (beam currents) and doses are shown in the D - Θ plane by Fig. 13.

From past experience (11), it was known that the beam showed a tendency to meander from target dosimeters in different trials. There were, therefore, chances of certain dosimeters not being hit by the beam properly. To allow for such losses of dosimeter samples, and to obtain good statistics from the data, it was decided to irradiate 4 sample packs in succession at each experimental point shown in Fig. 13. Data analysis after the experiment showed that the samples irradiated at the two higher doses at both the 1,000 and 2,000 mA/cm^2 beam current had to be discarded due to non-uniformity in beam charge density. Variation in beam size shifted the remaining experimental points from their planned positions. The points at the 40 mA/cm^2 beam

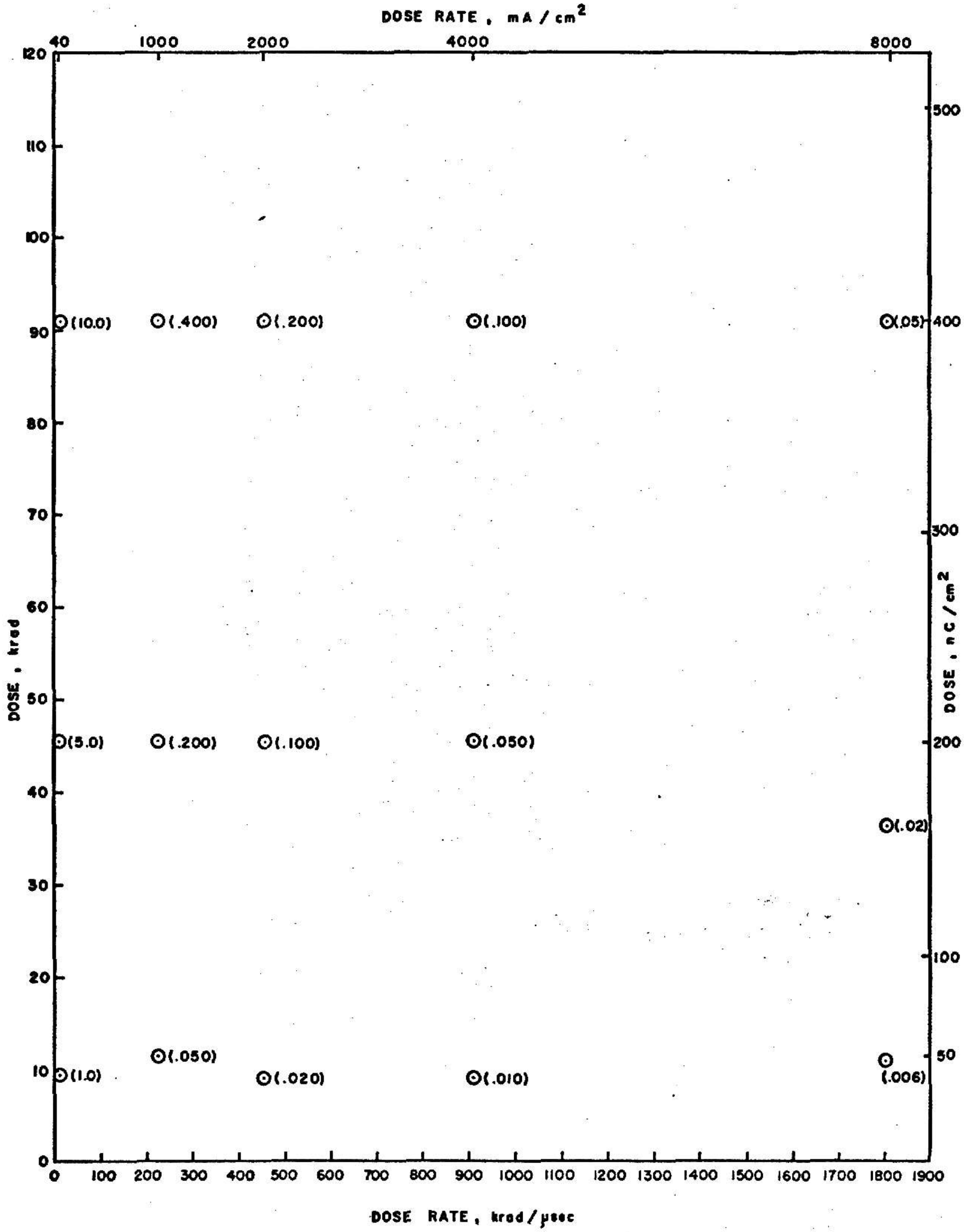

Fig. 13. Planned design of the experiment.

currents were shifted to higher doses and dose rates by approximately 25 %. All the remaining points were shifted to lower doses and dose rates by approximately 50 %. The actual experimental design obtained is shown in Fig. 14. Examination of Fig. 14 shows a somewhat distorted 3^2 factorial design. However, for our incomplete second order model a 2^2 factorial design with replicated center points would have been sufficient. Close examination of Fig. 14 shows several good 2^2 factorial designs with replicated center points. Therefore the actual design obtained would be expected to yield satisfactory results. The highest dose point at the 40 mA/cm^2 beam current appears to distort the design somewhat significantly so that data analyses were run both with and without this point. Since the results were not significantly changed either way, the results of the analysis without this point and hence better design are provided in the results of this investigation.

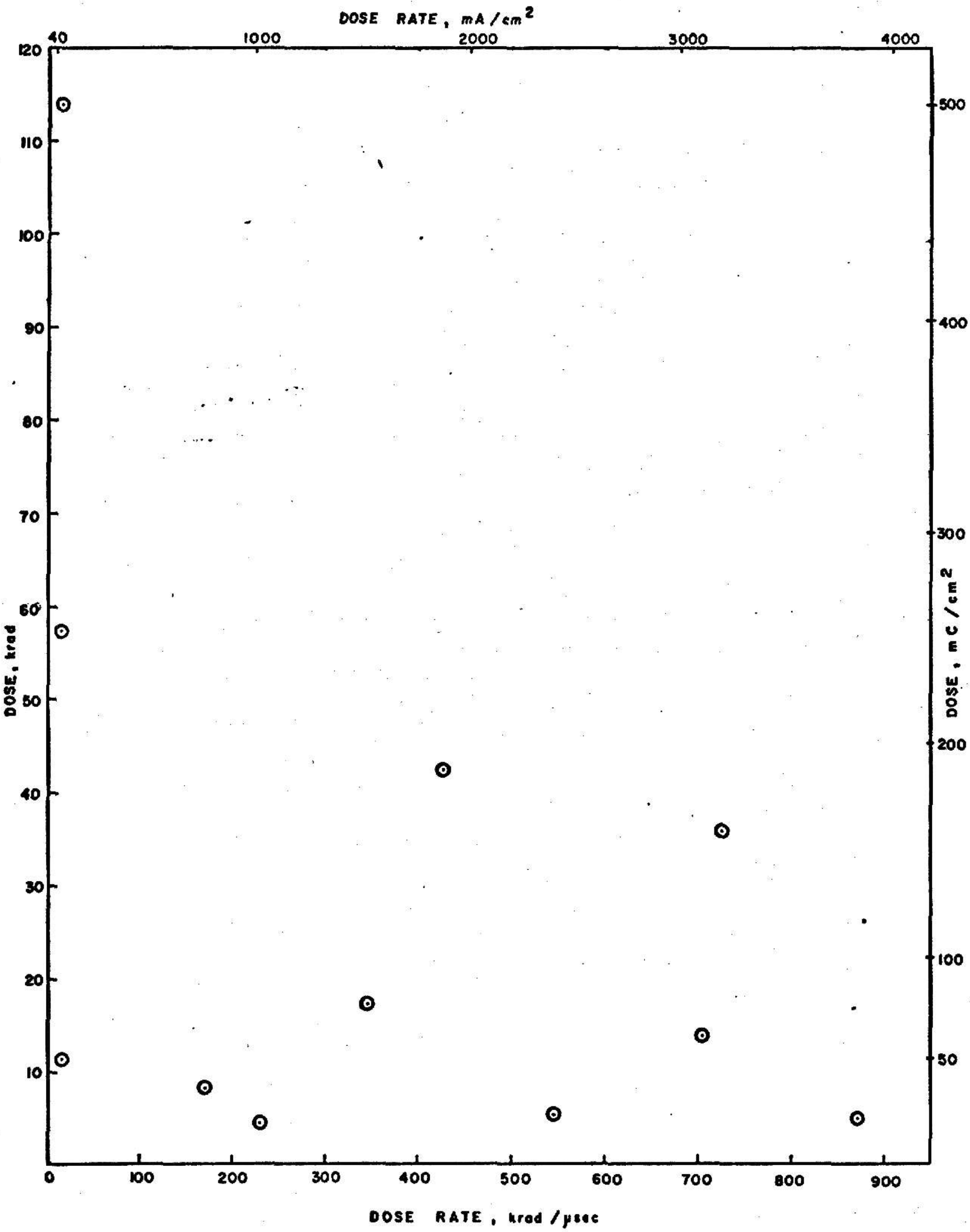

Fig. 14. Actual design of the experiment.

7. EXPERIMENTAL PROCEDURE

7.1. Electron Beam Monitoring:

The electron beam produced by the LINAC was tuned to be approximately 1 cm in diameter. The dosimeters were 0.6 cm in length, and previous studies had shown that the beam meandered from the target in different trials. Therefore it was important to know the beam position with respect to the dosimeters to determine whether they received the full dose they were expected to receive. To accomplish this, commercial dental x-ray film manufactured by the Rinn Corporation of Elgin, Illinois was mounted immediately behind the dosimeters. The shape of the beam along with a shadow of the dosimeters was obtained on the developed x-ray films (Fig. 22).

7.2. Preparation of Samples:

Physical size of the dosimeters was 0.9 mm diameter and 0.6 cm long. The electron beam was intended to have a circular cross section of 1 cm diameter and from previous experience it was known that the beam meandered primarily in the horizontal direction. Therefore, it was reasoned that six dosimeters mounted in a row in each trial would provide a reasonable probability that at least one dosimeter in each trial would be hit by the beam center. Dosimeter packages convenient to irradiate at the center beam port of the accelerator (Fig. 18) were made. These packages consisted of aluminum rings (5 cm outside diameter, 3 cm inside diameter, and 1/16 in thick), Rinn Super-1 dental x-ray film and six EG and G model TL-39 CaF_2:Mn thermoluminescent dosimeters which had been preannealed at 350^{o}C for 5 hours. The dosimeters used were those from which the points below 10^5 rad on the calibration curve of Fig. 11 were obtained. Sample numbers and perpendicular center lines were marked on the x-ray film packets. Six dosimeters were surrounded by a thin layer of polyethylene (Dow Saran Wrap) in order to keep them clean, and were taped at the center of an x-ray film packet using Permacel brand tape (New Brunswick, New Jersey). The x-ray films were cemented on the aluminum rings with Duco cement (E. I. DuPont deNemours and Company, Wilmington, Delaware). Sixty such packages were made. Serial numbers were marked on all samples at a particular position such that the position of this number served also as a reference point for describing the positions of the dosimeters in the sample. A view of a sample with a scale showing its size is shown in Fig. 16.

7.3. Sample Holding Device:

Alignment of the dosimeter packages on the center line of the electron beam was critical. To facilitate this and rapid sample changing at the accelerator the 3-jaw self-centering lens holding device shown in Fig. 17 was intended to be used. The jaws contained co-planar V-grooves in which the aluminum ring used in the sample could be seated. Two levers were provided to expand the jaws which were otherwise held close to the center by a spring. The outer ring of the holding device was provided with a fine ground radial rod which could be easily fixed in any stand on an optical bench.

Once the holding device was aligned with the beam, sample changing could be accomplished using the self-centering jaws without delay. Upon arrival at the accelerator site, it was discovered that a hydraulic line had been added near the top of the center beam part which precluded clearance for the self-centering holding device. Therefore, a smaller less sophisticated but satisfactory sample holding device available at the laboratory was used for the experiment.

The electron beam was horizontal. An optical bench, provided with the

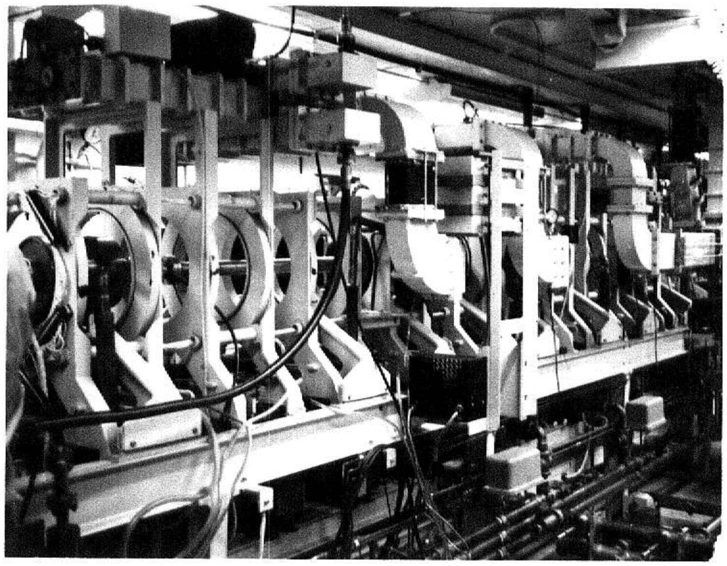

Fig. 15. A view from the injection end of the LINAC.

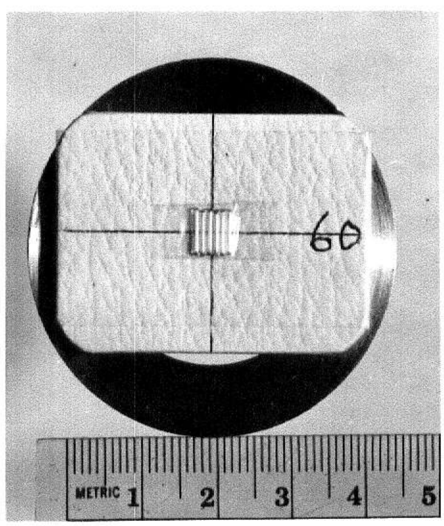

Fig. 16. Dosimeter sample for irradiation on the LINAC.

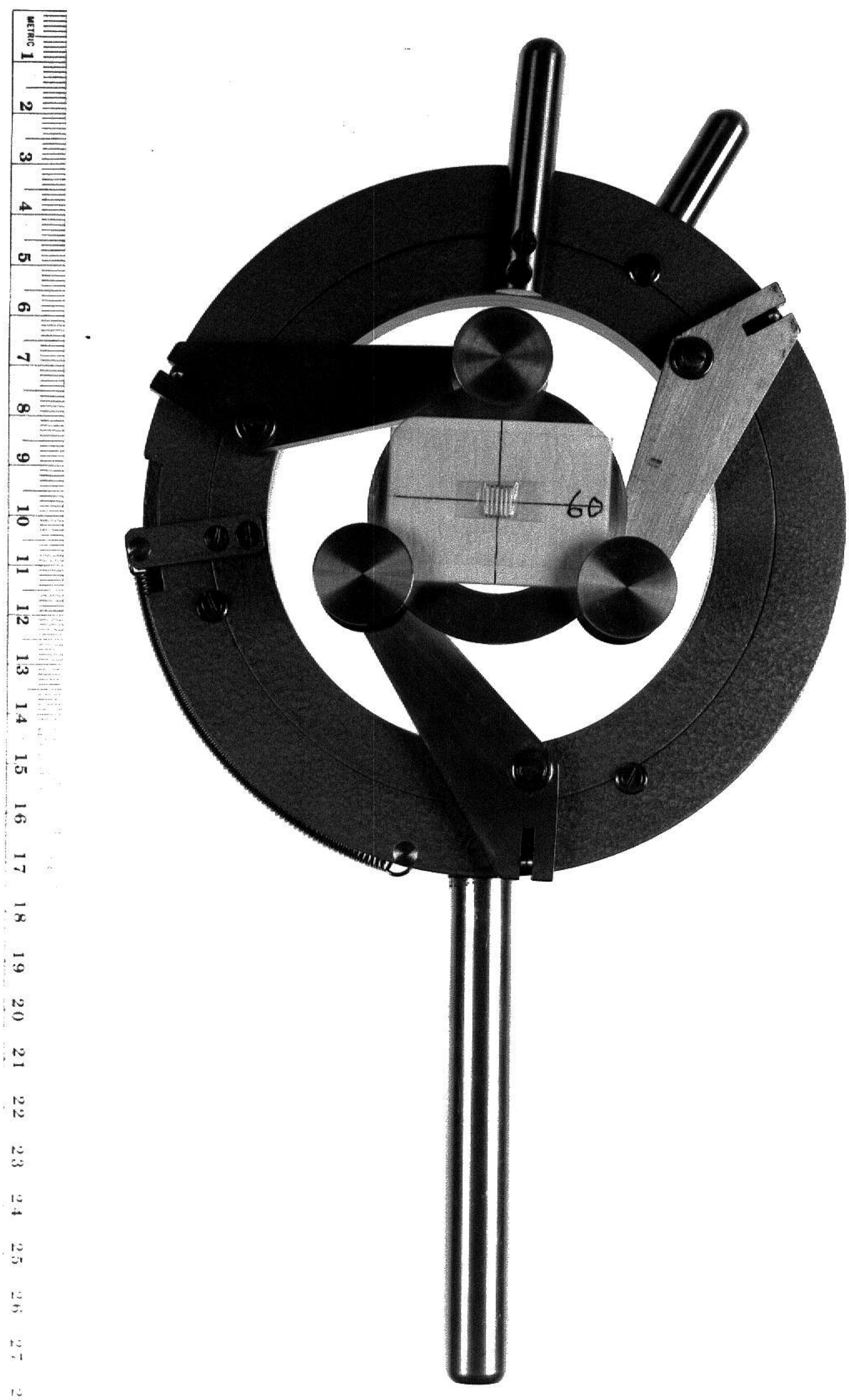

Fig. 17. Dosimeter sample in self-centering holding device.

accelerator as a standard accessory, was anchored horizontally with lead bricks in front of the beam port perpendicular to the axis of the beam. The holding device available at the laboratory was held in a stand on the optical bench close to the beam port such that its face was normal to the beam. A view of the irradiation assembly with the sample holding device in the optical bench is shown in Fig. 19.

Sample alignment packages were made by taping (with Permacel tape) pieces of ordinary glass microscope slides on some sample packages in place of the dosimeters. After the beam was tuned to the desired energy, amperage, pulse width, size, and approximate position one of the alignment packages was placed in the holding device and irradiated with the electron beam for about 20 pulses. The glass turned brown in the portion where it was hit by the electron beam. The position of this brown spot showed the position of the center point of the x-ray film packets in relation to the beam. Alignment was corrected by moving the optical bench and using the height adjustment screw on the holding device. Correct alignment of the sample was obtained by several such trials at each experimental point.

7.4. Irradiation of Samples:

The LINAC was operated by licensed operators of the Argonne National Laboratory. After the LINAC was tuned to the desired beam specifications and the sample holding device was aligned with the beam, a sample was mounted in the holding device. To record the relative positions of the six dosimeters in the sample, all the samples were mounted in a particular position which kept the dosimeters vertical and the sample number to the right as viewed from the injection end of the accelerator. The accelerator was pulsed once and a photograph of the oscilloscope trace of the pulse

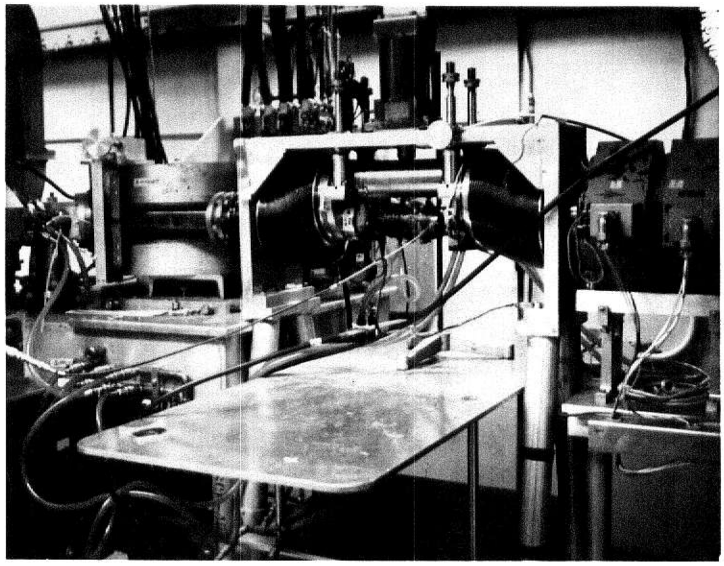

Fig. 18. A view of the center beam port on the LINAC.

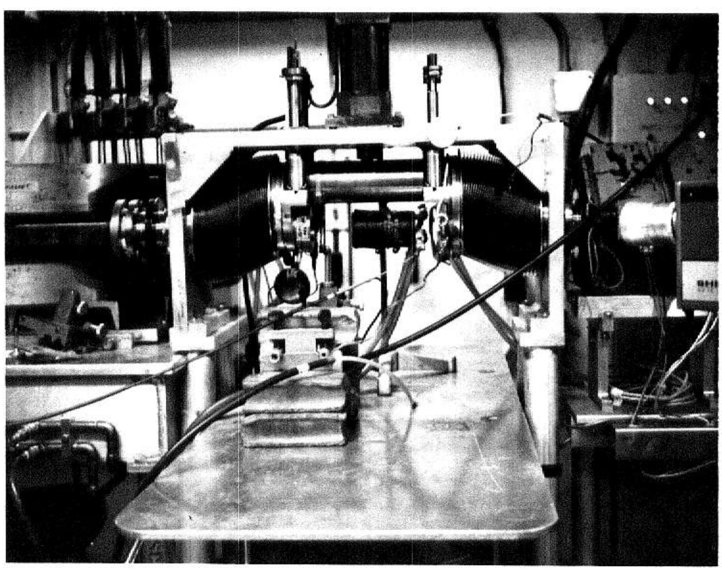

Fig. 19. A view of the irradiation assembly on the LINAC.

shape was taken. The sample number, the digital voltmeter reading and scale factor, and the scale factors for the oscilloscope screen were recorded. Another sample was then mounted in the holding device for irradiation. Following the same procedure, four dosimeter packages were irradiated at each setting of the accelerator given by the experimental design in Fig. 13. All sixty packages were irradiated over a time span of two days and nights.

7.5. Dosimeter Reading Procedure:

The dosimeter packages were brought back from Argonne National Laboratory to Manhattan, Kansas on the first day following the irradiations. On the second day, all the dosimeters were removed from the sample packages and placed in the graphite block holder carefully keeping track of each individual dosimeter. In ach package the dosimeters were numbered consecutively from the left toward the sample number marking. Near the end of the second day, all the dosimeters were simultaneously partially annealed at 161^{o}C for 7 min. On the third day, the responses of all the dosimeters were read. The high voltage on the dosimeter reader was set as described in section 4.2 in order to obtain the highest dose range at 50,000 reader units.

7.6. Determination of Dose and Dose Rate:

The total dose delivered to a dosimeter was proportional to the charge density supplied in the pulse. The total charge supplied in a pulse was determined from the digital voltmeter reading. The uniform charge density was then determined by dividing the total charge by the beam area. The conversion factor for a 1 cm^2 area beam was 0.227 krad (water)/nC (see sec. 6.2.). The dose rate was determined by dividing the total dose by the pulse width value obtained from the photograph of the pulse shape trace. A dosimeter would receive the calculated dose and dose rate only if the dosimeter was covered well by the beam and subjected to the uniform charge density. Previous experience with the LINAC (10) indicated that the charge density of the beam was not exactly uniform but varied only monotonically from the beam center to the edge. Assuming then that the charge density of the beam varied monotonically from the beam center to the edge, dosimeters centered on the centroid of the beam could then be said to have received a dose and dose rate proportional to that calculated for uniform charge density. To determine the beam area, and the dosimeter positions in the beam, and to provide a check on the uniformity of beam charge density the x-ray films in all packages were developed using standard x-ray film developing techniques. All the raw and computed data are presented in Appendix A.

8. ANALYSIS OF DATA

8.1. Pulse Shapes:

In order for the total dose to be delivered with a constant dose rate, the pulse shapes should have been rectangular. Typical pulse shapes produced by the LINAC at pulse widths of 10, 0.05, and 0.02 μsec are shown in Fig. 20. The pulse shapes are seen to be reasonably rectangular.

8.2. Electron Beam Energy Spectra:

In order to preclude the introduction of another variable, electron energy, a monoenergetic beam of 15 MeV electrons was intended to be used. As a check on the electron energy, electron beam energy spectra were requested from the LINAC operators. Typical electron beam energy spectra produced by the LINAC at beam currents of 40 mA/cm^2, 4 A/cm^2, and 8 A/cm^2 are shown in Fig. 21. The electron beams are seen to be reasonably monoenergetic at 15 MeV.

8.3. Sorting of the Dosimeters:

The developed x-ray films permitted several observations. The size and shape of the electron beam varied from the desired 1 cm diameter circular shape. It was also obvious in some cases that the charge density in the beam did not vary monotonically from the beam center to the edge. Beam meandering was not significant, so that each sample contained at least one dosimeter approximately centered on the centroid of the beam image. Some of the typical developed films are qualitatively reproduced in Figs. 22 and 23. Samples in which the charge density obviously did not vary monotonically from the center such as sample numbers 15, 20, 21, and 30 were discarded. The dosimeter response selected for the remaining samples was

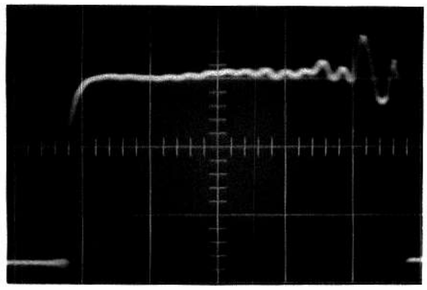

(a) 10 μsec

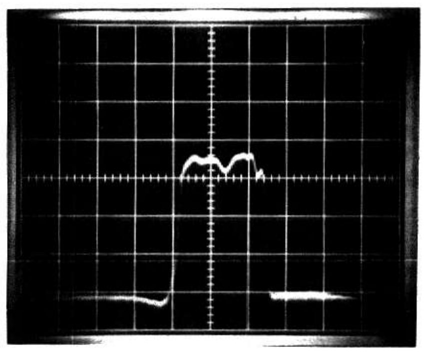

(b) 0.05 μsec

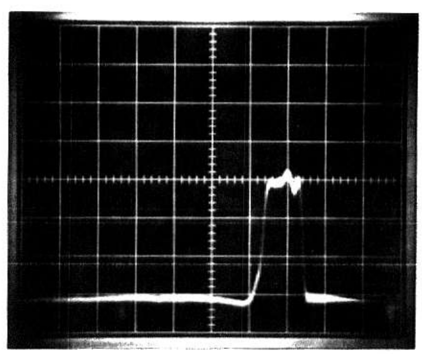

(c) 0.02 μsec

Fig. 20. Typical electron beam pulse shapes for various pulse widths.

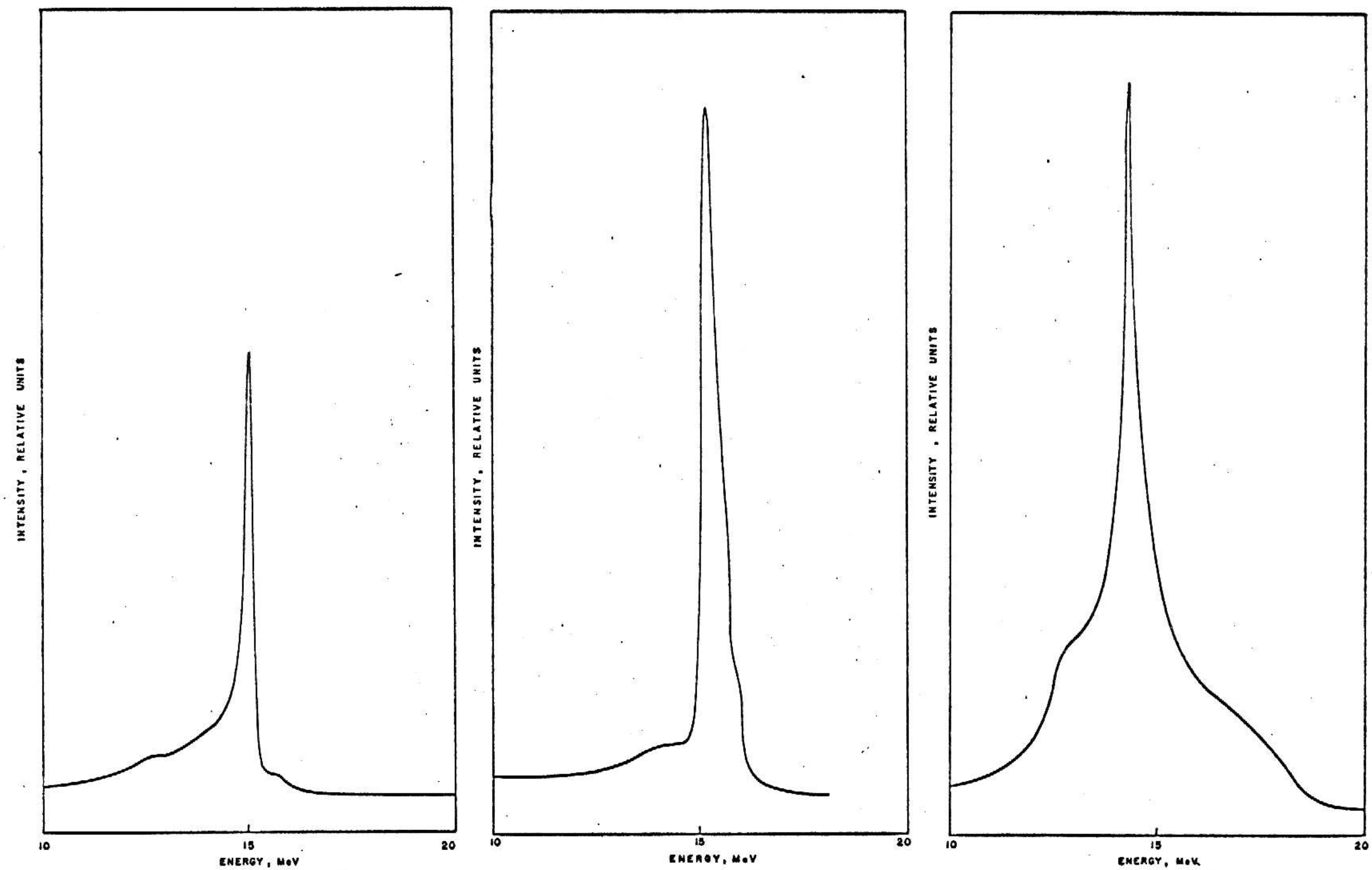

(a) 40 mA/cm^2 (b) 4 A/cm^2 (c) 8 A/cm^2

Fig. 21. Typical electron beam energy spectra for various beam currents.

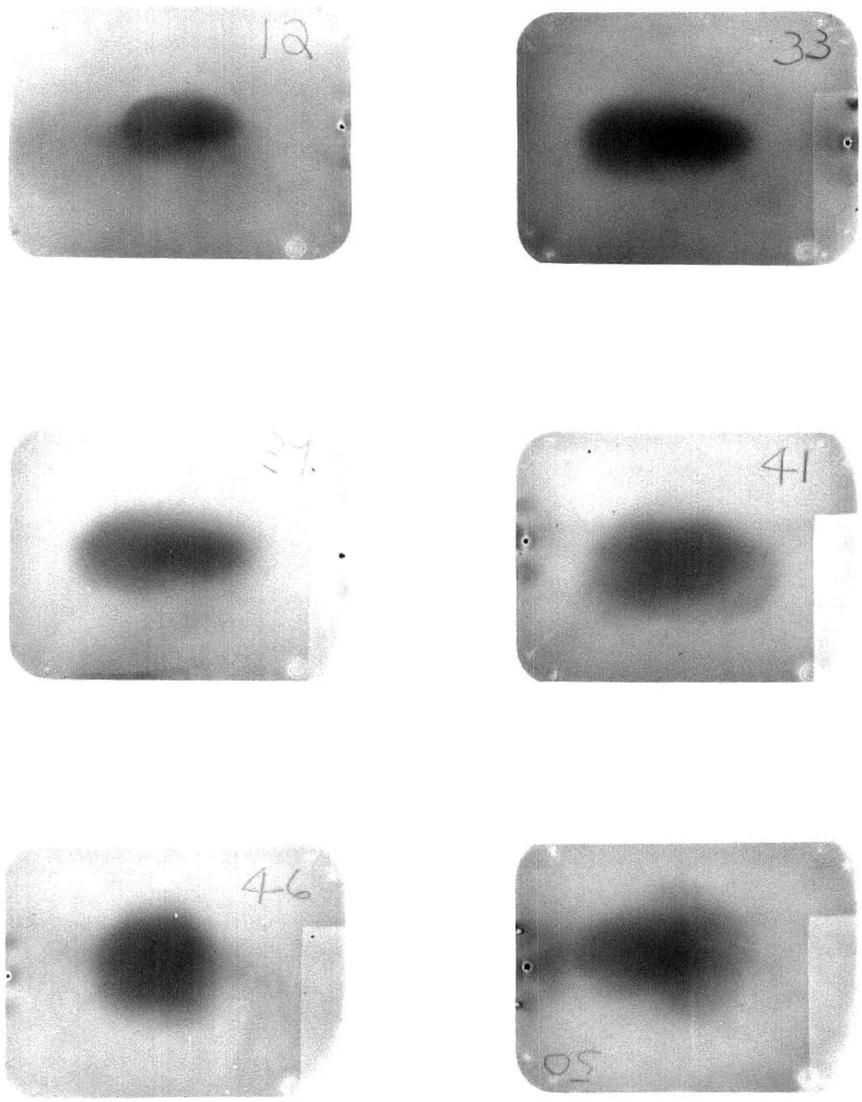

Fig. 22. Typical developed x-ray films.

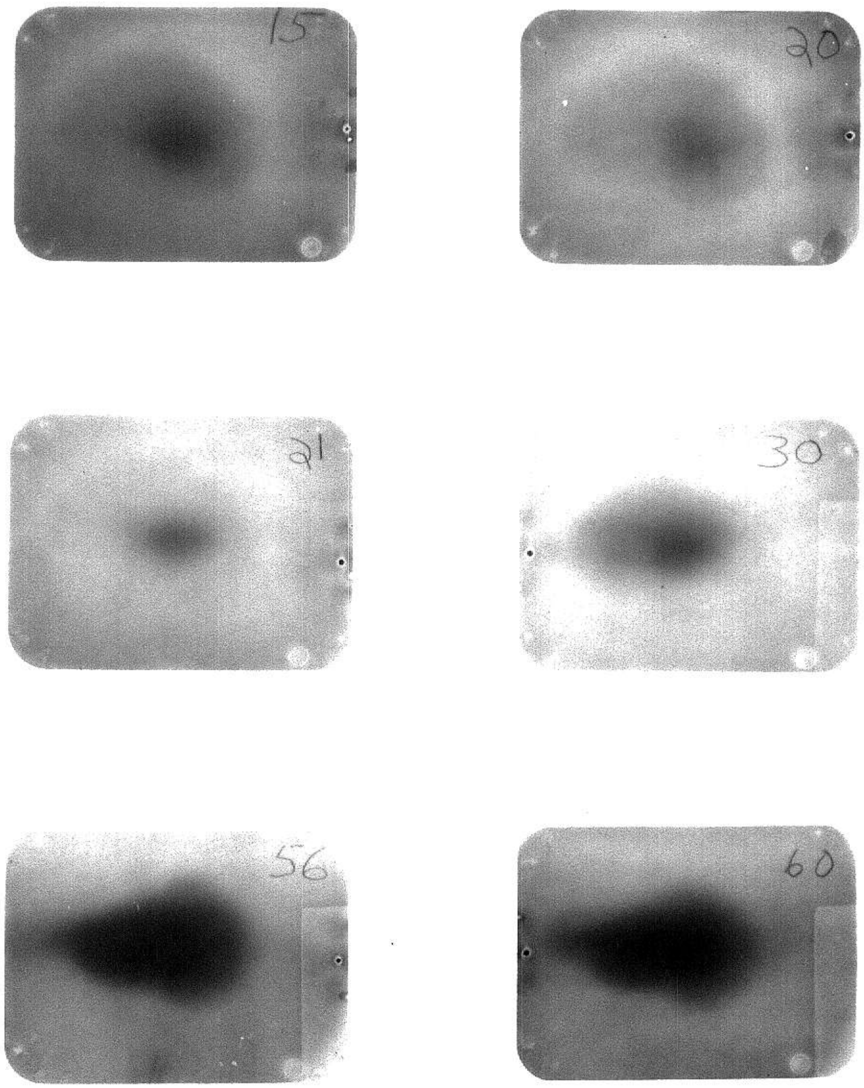

Fig. 23. Typical developed x-ray films.

the dosimeter centered on the estimated centroid of the beam image which in nearly all cases corresponded with the highest response in the sample. For the samples retained for data analysis, the films indicated that the charge density of the beams varied only monotonically from the center. This was further evidenced by the responses of the remaining dosimeters in the sample, provided they did not closely approach the edge of the beam.

8.4. Data Analysis:

All the experimental points whose samples were not discarded for reasons given in the preceding section are shown in Fig. 14. As indicated in section 6.3, the data were analyzed with and without the highest dose point at the 40 mA/cm^2 beam current because of its apparent design distortion and proximity to the saturation response range. Since the results were not significantly changed either way, the results of the analysis without this questionable point are provided in this investigation. All the data utilized for the results contained in this section are listed in Appendix A. The mathematical model selected for data analysis was:

$$R = R_{00} + R_{10}D + R_{01}\Theta + R_{11}D\Theta$$

Should there be no effect of the high dose rates used in the experiment on the response of the dosimeters, dosimeter response would be dependent only on the dose received by the dosimeters. In such a case data analysis would yield: $R_{01} = 0$, $R_{11} = 0$ and $R_{10} \neq 0$. On the other hand if the response was affected by the high dose rates, data analysis would yield the coefficients R_{01} and R_{11} different from zero; greater or less than zero depending upon the effect of the high dose rates.

The constant coefficients R_{00}, R_{01}, R_{10} and R_{11} were evaluated by performing a regression analysis of the data using the "Forward Doolittle

Technique" described by Hunter (17). A more general discussion of this technique can be found in the reference by Draper and Smith (18). The values of D and Θ used in the analysis were the total dose and dose rate values which the dosimeters would have received had the charge density of the beam been uniform. Since the absolute dose and dose rate received by the dosimeters were assumed proportional to the uniform values, the qualitative nature of the results obtained would not be affected by the lower values of D and Θ used. To keep the numbers in reasonable magnitudes the dose values were expressed in units of krad and the dose rates in units of krad/μsec. Statistical significance of the results was determined by applying the F-test on the values of coefficients determined. Results along with the calculated F-ratios and critical F-ratios are presented in Table III. The values of the critical F-ratios were obtained from Draper and Smith (18).

8.5. Results:

Using the equation:

$$R = R_{00} + R_{10}D + R_{01}\Theta + R_{11}D\Theta \qquad (8.5)$$

the data analysis yielded:

$$R_{00} = 98.5 \text{ (reader units)}$$

$$R_{10} = 49.5 \text{ (reader units/krad)}$$

$$R_{01} = -0.378 \text{ (reader units/krad } \mu\text{sec}^{-1})$$

$$R_{11} = 0.101 \text{ (reader units/krad}^2\ \mu\text{sec}^{-1})$$

The coefficients of Θ and of the interaction term ($D\Theta$) were seen to be significantly different from zero at the 99.9 % confidence level. Hence the dose rate dependence of the response of EG and G model TL-39 dosimeters was proved. The results obtained were only of a qualitative nature since the actual dose and dose rates received by the dosimeters were not exactly

Table III. Results of regression analysis.

Regression parameter	Value	Calculated F-ratio	Critical F-ratio	Confidence level
R_{00} (reader units)	98.5	--	--	--
R_{10} (reader units/krad)	49.5	--	--	--
R_{01} (reader units/krad μsec^{-1})	-0.378	154	7.43	99.9 %
R_{11} (reader units/krad^2 μsec^{-1})	0.101	213	7.43	99.9 %

known on an absolute scale.

8.6. Presentation of Results:

Equation (8.5) represents a surface in the R-D-Θ space. The projection on the R-Θ plane of this response surface in the range investigated together with the projections of the experimental points and their calculated response values on the response surface using equation (8.5) are shown in Fig. 24. Most of the experimental points lie very close to their calculated response value on the surface showing that the model fits the experimental data rather well. From equation (8.5) it can be seen that at a constant dose (D), the response (R) becomes a linear function of the dose rate (Θ). The projections of these so called isodose lines on the R-Θ plane are also shown. From this type of plot knowing any two of the three variables, R-D-Θ, one can obtain the value for the third variable. Another advantage of this type plot is the clear picture of the dose rate effect on the response at various dose levels. The dependence of the dose rate effect on dose is also clearly shown.

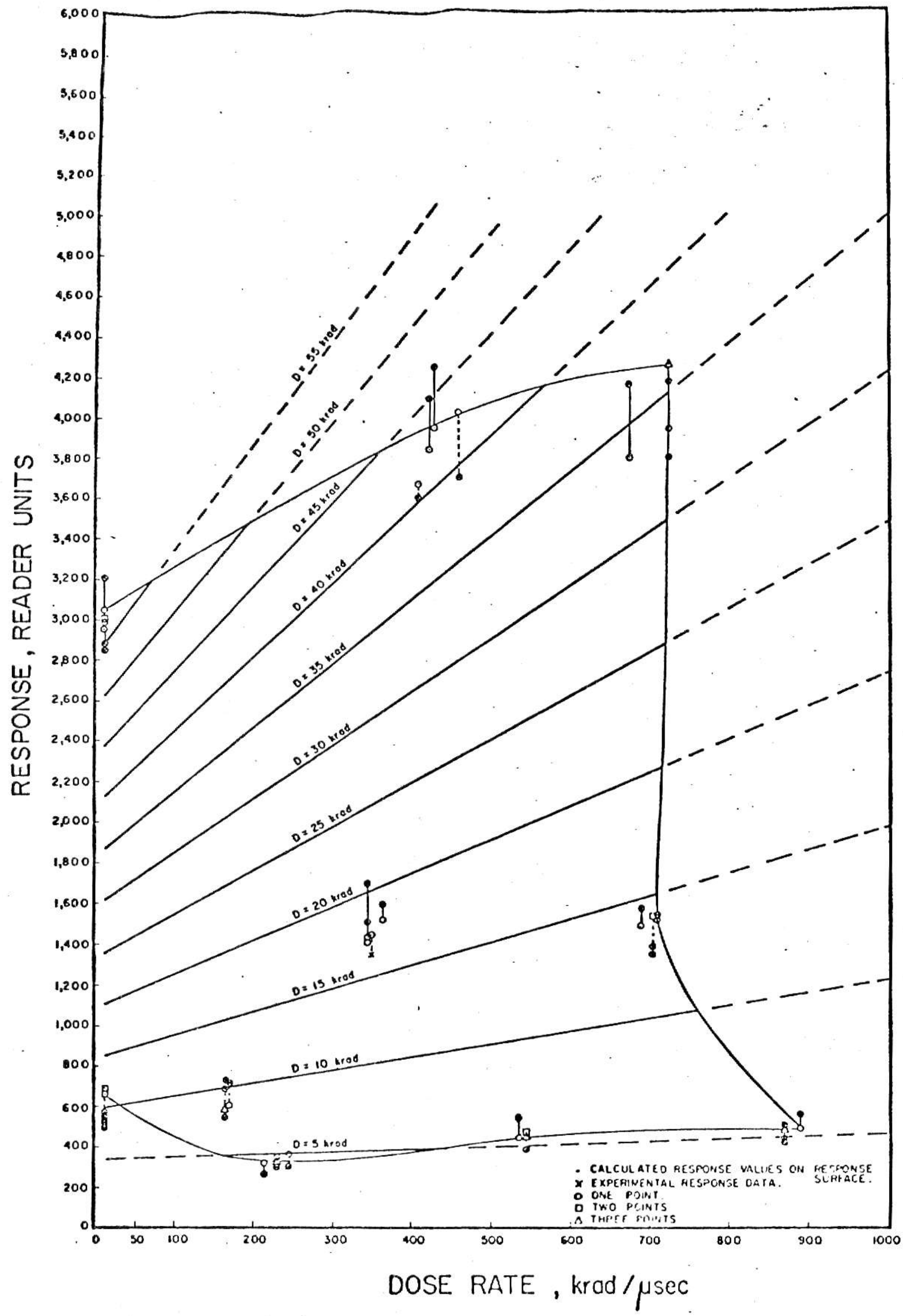

Fig. 24. Response of CaF_2:Mn dosimeters to varying dose and dose rate.

9. DISCUSSIONS AND CONCLUSIONS

9.1. Discussion of Results:

The coefficient R_{01} of Θ in the response equation has been shown to be significantly different from zero at the 99.9 % confidence level. This is sufficient to say decisively that the response of EG and G model TL-39 CaF_2:Mn TL dosimeters is dose rate dependent. Further the coefficient R_{11} of the interaction term ($D\Theta$) is also significantly different from zero at the 99.9 % confidence level. Donnert's theory says that if the response is dose rate dependent, the coefficient R_{11} should also be different from zero. Thus the data and Donnert's theory are in agreement. From Donnert's theory it may also be said that the mechanism of irradiation of CaF_2:Mn involves processes which are other than first order kinetically.

Only a particular type of CaF_2:Mn dosimeters, namely the EG and G model TL-39, were used in this study. But none of the limitations placed on the dosimeters due to their physical structure and size was surpassed in the experiment. Therefore the qualitative results obtained by this experiment might be expected to hold in general for any kind of CaF_2:Mn dosimeters. The dose levels and dose rates at which the dose rate effect becomes significant might change with the type of dosimeter but the general qualitative features determined in this experiment should not be expected to change.

Looking at Fig. 24, wherin some isodose lines are shown, two facts are to be noticed:

(1) the slopes of all the isodose lines are positive;

(2) different isodose lines have different slopes, and the slopes increase with increasing dose level; showing that the dose rate dependence

is characteristic of the total dose supplied to the dosimeter. This means that the dose rate dependence is also a function of the dose already supplied to the dosimeter.

Referring to Cameron's model of thermoluminescence described briefly in section 2.2.4., the following statements concerning the proposed hypothesis of the creation of traps by radiation can be made in the light of the results of this research:

(1) the proportionality constant for the creation of traps is a function of dose rate;

(2) the proportionality constant for the creation of traps is also a function of the dose already supplied to the dosimeter.

9.2. Previous Investigations and Results:

By means of a 3-MV x-ray system Tochilin and Goldstein (4) studied the dose rate effect on the response of CaF_2:Mn dosimeters using dose rates up to 10^{11} rad/sec and doses up to 4,500 rad. They reported the response independent of dose rate within the accuracy of the experiment (10 %). Their results are in agreement with the results of this investigation in their range of dose rates and total dose. The conclusions of this study are that CaF_2:Mn dosimeters are affected by dose rate in the range of 10^{10} to 10^{12} rad/sec with doses in the range of 5 to 60 krad.

9.3. Conclusions:

There were two main conclusions drawn from these studies.

(1) Within the dose and dose rate ranges of this investigation, the response of the CaF_2:Mn thermoluminescent dosimeter is an increasing function of the rate at which the radiation dose is delivered to it. For EG and G model TL-39 dosimeters the dose rate dependence is observeable in the dose

range from approximately 5 krad to 60 krad and in the dose rate range from approximately 10 krad/μsec to 900 krad/μsec.

(2) The dose rate dependence of CaF_2:Mn thermoluminescent dosimeter is itself an increasing function of the total dose delivered to the dosimeter. Another conclusion drawn based on Donnert's theory is:

(3) The kinetic order of the processes involved in the irradiation of CaF_2:Mn phosphor is different from first order.

10. LIMITATIONS OF THE CURRENT INVESTIGATION

Limitations faced in this investigation were primarily from the radiation facility. The LINAC was the only radiation facility within comparatively easy reach that could be used in the experiment, but the practical limitations faced suggest that a more sophisticated radiation facility should be sought in order to obtain accurate quantitative results. Quantitative results could have been obtained for the TL-39 dosimeters if the absolute dose and dose rates delivered to the dosimeters could have been ascertained. These absolute values could have been determined if the charge density of the beam had been uniform. With the LINAC this problem seems inherent. Perhaps the situation could be improved by focusing techniques or by some device capable of measuring the charge supplied to an individual dosimeter such as a chambered Faraday cup.

A confirming but insufficient check on the dosimetry techniques of this investigation can be made by comparison of the calculated uniform dose with the dose obtained from the calibration curve for a given sample. This comparison could be valid only in the low dose rate range (10^{10} rad/sec) where Tochilin and Goldstein (4) observed no dose rate effect. Agreement between the calculated dose and the calibration curve dose for a given response would be expected under the following conditions:

1. The dosimeter response to ^{60}Co gamma radiation is equivalent to the response to 15 MeV electrons.

2. There is no observable dose rate effect at the lowest dose rate investigated (10^{10} rad/sec).

3. The charge density of the beam is uniform.

4. The conversion factor of 0.227 krad/nC for a 1 cm^2 beam is valid.

5. The variance in the response of the dosimeters at any given dose is negligible.

6. The net effect of departure from conditions 1 through 5 is zero.

The comparison of these results for the samples irradiated at the lowest dose rate (10^{10} rad/sec) is shown in Table IV. Both the agreement between the dose obtained from the calibration curve and the calculated uniform dose and the consistency of the ratios of the two are remarkable. The consistency of the ratios of the calibration curve dose to the calculated uniform dose tends to confirm the assumption that the actual dose received by the dosimeter on the beam centroid is proportional to the calculated uniform dose.

Table IV. Comparison of the calculated uniform dose with the dose obtained from the calibration curve.

Sample number	Response, reader units	Dose from calibration curve, krad	Calculated uniform dose, krad	Ratio of calibration curve dose to calculated dose
1	5,200	123	114	1.08
2	5,200	123	112	1.10
3	5,500	131	113	1.16
4	5,000	118	113	1.05
5	2,850	63.2	58.4	1.08
6	2,880	63.3	56.5	1.12
7	3,000	66.5	57.5	1.16
8	3,210	70.5	57.5	1.22
9	540	14.0	11.8	1.18
10	520	13.6	11.7	1.16
11	570	14.7	11.1	1.32
12	494	13.2	11.3	1.17

11. SCOPE FOR FUTURE WORK

There is a vast scope of work to be done in the field of thermoluminescent dosimetry whose practical value seems to be great.

Further work that may be done in the specific direction of studying the dose rate dependence obviously includes obtaining some quantitative results which may be of practical use. The tasks to be faced in this particular work will be gaining access to a radiation facility which is more sophisticated than LINAC, or developing a device for measuring the charge supplied by the LINAC to an individual dosimeter. Quantitative dose rate studies in this dose rate range could then be expanded to other phosphors throughout the general field of thermoluminescence.

Another area of investigation is the supralinearity observed in the calibration curve. The differences and similarities between the calibration curve obtained in this study and that obtained by Alexander (16) are not readily explainable and would be of interest for an investigation. Included in this area could be the effect of dose rate on supralinearity.

The effects of saturation including the type and extent of any radiation damage is another area for further study. Included in this area could be the effect of dose rate on saturation. Low temperature studies on the CaF_2:Mn phosphor is another area which may offer clues to the mechanism of TL.

In the general field of thermoluminescence of CaF_2:Mn, the main problem of the determination of the detailed mechanisms of irradiation and light emission still remains unsolved. Without knowledge of the actual mechanism of thermoluminescence, it is unsafe to extrapolate any of the experimental facts.

12. ACKNOWLEDGMENTS

The author is indebted to a number of people: to Dr. Hermann J. Donnert for his valuable suggestions and continuous help from selection of the topic for research through physically assisting in the actual experimental work at Argonne National Laboratory to finishing the thesis; to Mr. George Mavrogenes, Mr. B. E. Clifft, Mr. P. T. Ficht, and Mr. J. M. Kielbasa of the Electron Linear Accelerator Section at Argonne National Laboratory; to Mr. Ray E. Hightower for assistance with the experimental equipment; to Mr. George Abshires for assistance with equipment fabrication; to Dr. Dragsdorf for assistance with the x-ray film development; to Mr. Albert Alexander and Mr. Oliver Block for their experienced advice and assistance; to my wife, Nancy for her assistance in typing the final thesis copy; and to my daughter, Kim for her cheering encouragement. The author wishes to thank them all. The financial support from the Department of Defense Themis Project administered through the Office of Naval Research and from the Department of the Army which supported the author's studies at Kansas State University are gratefully acknowledged.

13. LITERATURE CITED

1. Cameron, J. R., Suntharalingam, N., and Kenney, G. N., Thermoluminescent Dosimetry (The University of Wisconsin Press, 1968).

2. Ginther, R. J., and Kirk, R. D., "The Thermoluminescence of CaF_2:Mn," J. Electrochem. Soc. 104, 365 (1957).

3. Schulman, J. H. et al, "New Thermoluminescent Dosimeter," Rev. Sci. Instr. 31, 1263 (1960).

4. Tochilin, E. and Goldstein, N., "Dose Rate and Spectral Measurements from Pulsed X-ray Generators," Health Phys. 12, 1705 (1966).

5. Schulman, J. H., "Survey of Luminescence Dosimetry," Luminescence Dosimetry, ed. F. H. Attix, (U. S. Atomic Energy Commission, Division of Technical Information, Oak Ridge, Tennessee, 1967), 7.

6. Randall, J. T. and Wilkins, M. H. F., "Phosphorescence and Electron Traps," Proc. Roy. Soc. (London) A 184, 366 (1945).

7. Bonfiglioli, G., Brovetto, P. and Cortese, C., "Thermoluminescence and F-Centers," Phys. Rev. 114, 951 (1959).

8. Hill, J. J. and Schwed, P., "Experimental Study of the Mechanism of Thermoluminescence in Irradiated NaCl," J. Chem. Phys. 23, 652 (1955).

9. Cameron, J. R., Zimmerman, D. W. and Bland, R. W., "Thermoluminescence Vs. Roetgens in LiF: A Proposed Mathematical Model," Luminescence Dosimetry, ed. F. H. Attix, (U. S. Atomic Energy Commission, Division of Technical Information, Oak Ridge, Tennessee, 1967), 47.

10. Donnert, H. J., Klein, N. and Sassé, R. A., "The Response of Selected Gamma Radiation Detectors to Radiation Delivered at Very High Dose Rates," (Paper presented at the Army Science Conference, U. S. Military Academy, West Point, New York, 1964), (Classified).

11. Kaiseruddin, M., "Effects of Very High Dose Rates on the Response of LiF Thermoluminescent Dosimeters," (Unpublished M. S. Thesis, Kansas State University, 1968). Also, Donnert, H. J., and Kaiseruddin, M., "Response Kinetics of LiF Thermoluminescent Dosimeters," Bull. Am. Phys. Soc. 15, 1367 (1970).

12. Pinkerton, A., Holt, J. G., Laughlin, J. S., Almond, P. R., "Direct Intercomparison of Absorbed Dose by Thermoluminescent Dosimetry," Luminescence Dosimetry, ed. F. H. Attix, (U. S. Atomic Energy Commission, Division of Technical Information, Oak Ridge, Tennessee, 1967), 363.

13. Nash, A. E., Attix, F. H., and Schulman, J. H., "Spurious Thermoluminescence of CaF_2:Mn and LiF (TLD-100)," Luminescence Dosimetry, ed. F. H. Attix, (U. S. Atomic Energy Commission, Division of Technical Information, Oak Ridge, Tennessee, 1967), 244.

14. Schayes, R., Brooke, C., Kozlowitz, I., and Lheureux, M., "Thermoluminescent Properties of Natural Calcium Fluoride," Luminescence Dosimetry, ed. F. H. Attix, (U. S. Atomic Energy Commission, Division of Technical Information, Oak Ridge, Tennessee, 1967), 138.

15. TL Dosimetry System, Models TL-3B and TL-3C, Operation Manual, # S-316-MN, (EG and G, Santa Barbara Division, 1966).

16. Alexander, A. J., "The Response Characteristics of CaF_2:Mn Thermoluminescent Dosimeters," (Unpublished M. S. Thesis, Kansas State University, 1970).

17. Hunter, J. S., Response Surface Methodology, (NDL-SP-1, Nuclear Defense Laboratory, Army Chemical Center, Maryland, 1962).

18. Draper, N. R., and Smith, H., Applied Regression Analysis, (John Wiley and Sons, Inc., 1966).

APPENDIX A

Table V. Raw and compulted data from irradiation on the LINAC

Sample number	Total charge, nC	Beam area, cm^2	Total dose, krad	Pulse width, μsec	Dose rate, krad/μsec	Response, reader units	Calculated response, reader units
1	377	0.75	114	10.0	11.4	5,200	--[a]
2	370	0.75	112	10.0	11.2	5,200	--[a]
3	373	0.75	113	10.0	11.3	5,500	--[a]
4	373	0.75	113	10.0	11.3	5,000	--[a]
5	193	0.75	58.4	5.0	11.6	2,850	3,050
6	187	0.75	56.5	5.0	11.3	2,880	2,960
7	190	0.75	57.5	5.0	11.5	3,000	3,010
8	190	0.75	57.5	5.0	11.5	3,210	3,010
9	39.0	0.75	11.8	1.0	11.8	540	692
10	38.7	0.75	11.7	1.0	11.7	520	688
11	36.7	0.75	11.1	1.0	11.1	570	656
12	37.3	0.75	11.2	1.0	11.2	494	666

[a] Data not included in the data analysis (Sec 8.4).

Table V. (Continued)

25	327	1.7	43.6	0.10	436	3,700	4,020
26	307	1.7	40.9	0.10	409	3,600	3,670
27	317	1.7	42.3	0.10	423	4,090	3,840
28	323	1.7	43.1	0.10	431	4,250	3,950
33	287	1.8	36.1	0.050	723	4,180	4,260
34	267	1.8	33.6	0.050	673	4,160	3,800
35	287	1.8	36.1	0.050	723	3,940	4,260
36	287	1.8	36.1	0.050	723	3,800	4,260
37	143	2.3	14.1	0.020	705	1,390	1,530
38	140	2.3	13.8	0.020	690	1,580	1,480
39	143	2.3	14.1	0.020	705	1,350	1,530
40	144	2.3	14.2	0.020	710	1,530	1,550
41	46.0	2.0	5.22	0.0060	870	428	485
42	47.0	2.0	5.22	0.0060	870	500	485
43	47.0	2.0	5.33	0.0060	889	570	504
44	46.0	2.0	5.22	0.0060	870	442	485
45	45.7	1.9	5.45	0.010	545	470	462
46	45.7	1.9	5.45	0.010	545	482	462

Table V. (Continued)

47	44.7	1.9	5.34	0.010	534	550	448
48	45.7	1.9	5.45	0.010	545	388	462
49	166	2.2	17.1	0.050	342	1,510	1,410
50	168	2.2	17.3	0.050	346	1,700	1,430
51	176	2.2	18.1	0.050	363	1,600	1,520
52	169	2.2	17.4	0.050	348	1,350	1,440
53	49.3	2.3	4.86	0.020	243	312	366
54	46.3	2.3	4.56	0.020	228	308	343
55	43.7	2.3	4.31	0.020	215	270	324
56	46.3	2.3	4.56	0.020	228	342	343
57	85.0	2.3	8.38	0.050	167	690	592
58	85.0	2.3	8.38	0.050	167	730	592
59	85.3	2.3	8.41	0.050	168	550	594
60	87.3	2.3	8.61	0.050	172	720	609

EFFECTS OF VERY HIGH DOSE RATES ON THE RESPONSE OF CALCIUM FLUORIDE THERMOLUMINESCENT DOSIMETERS

by

JAMES DAVID SMARSH

B. S., University of Kansas, 1961

AN ABSTRACT OF A MASTER'S THESIS

submitted in partial fulfillment of the

requirements for the degree

MASTER OF SCIENCE

Department of Nuclear Engineering

KANSAS STATE UNIVERSITY
Manhattan, Kansas

1971

ABSTRACT

The theory of thermoluminescence and pertinent thermoluminescent dosimetry for the EG and G model TL-39 CaF_2:Mn Microthermoluminescent Dosimeters were briefly reviewed. A calibration curve for the TL-39 dosimeters was experimentally determined with ^{60}Co gamma rays for the dose range of 100 to 1.5×10^6 rad.

To obtain dose rates of the order of 10^{10} to 10^{12} rad/sec the Electron Linear Accelerator at the Argonne National Laboratory was used. A 15 MeV electron beam was used to irradiate the dosimeters. Total doses of the order of 10^4 rad were supplied in single pulses of widths of the order of μsec.

Data were analyzed by a regression procedure. The conclusions drawn were: (1) the response of CaF_2:Mn dosimeters is dependent upon the dose rate of delivered radiation in the dose rate range of approximately 10^{10} to 10^{12} rad/sec and in the dose range of about 5 to 60 krad; (2) the dose rate effect is a dose dependent phenomenon; and (3) the kinetic order of the processes involved in the irradiation of CaF_2:Mn is other than unity.